Diff of AWS

CALCULATION OF HEAT PROCESSES IN WELDING

1960

Prof. Dr. N.N. Rykalin

M o s c o w , U. S. S. R.

Paper given 42nd Annual Mtg. of American Welding Society, 1960 Educational Series

(Information from Mr. Lessley 11/19/63)

CALCULATION OF HEAT PROCESSES IN WELDING

1960

Prof. Dr. N.N.Rykalin

M o s c o w , U. S. S. R.

Calculation of Heat Processes in Welding

Preface

The welding processes in metals proceed in most cases with a quick change of temperatures within the range of from the ambient air temperature to the temperature which equals sometimes to that of the metal evaporation.

Various physical and chemical processes take place in this temperature range which is rather broad. These processes are as follows: the melting of base and filler metals, metallurgical reactions in molten pool, the crystallisation of molten metal, structural and volumetric changes in the weld metal as well as in the parent metal, phenomena of local plastic strain.

In order to regulate welding processes it is necessary to know how they are affected by all the essential parameters including the temperature change in the course of time.

The heating and cooling processes in metals during welding as well as during local heat treatment are defined by the influence of highly concentrated heat sources and the conditions of heat flow from regions where these sources are acting. The electric arc, gas flame and electric current applied to the contact area of the surface of a workpiece as well as friction in this area - all can produce local heat. The heat these sources generate is distributed very

unevenly over the surface or throughout the volume of the metal.

Heat sources used in welding are characterized by the effective thermal power which is the amount of heat generated in or introduced to the metal per unit of time, and by its distribution over the surface or throughout the volume of metal.

Heating of Metals by Welding Arc

T h e r m a l c h a r a c t e r i s t i c s o f t h e w e l d i n g a r c. The total thermal power of the welding arc is assumed to be approximately equal to the thermal equivalent of its electric power (0.24 UJ cal/sec, where U - voltage drop across the arc in V; J - current in A) although chemical reactions in the arc gap may alter somewhat the thermal balance of the welding arc.

The effective thermal power q of the welding arc is the amount of heat generated in or introduced to the metal of the workpiece and consumed in heating it up

$$q = 0.24\eta_u UJ \qquad (1)$$

Efficiency η_u of the heating process is the ratio of heat, introduced in the workpiece by the welding arc, to the thermal equivalent of the electric power of this arc. This coefficient defines the effectiveness of heat generation and of heat exchange in the arc gap and it depends upon technological conditions of welding.

By comparing the change of the heat content in metal, being measured in a water calorimeter, with electric power consumption in the welding circuit it was found that the efficiency η_u varies from 70 to 85% in open arc metal electrodes welding, from 80 to 95% in submerged arc welding, and from 50 to 75% in carbon electrodes welding. Efficiency decreases with the lenghtening of the welding arc and

increases somewhat with the deepening of the arc in the puddle.

When metal electrodes are used efficiency doesn't vary appreciably with welding current, its kind and polarity. The heat flux of the welding arc has the maximum intensity at the central part of the hot spot where heat is generated directly over the surface layer of metal due to the electronic and ionic bombardment.

In the annular zone surrounding the electrically active spot the metal is heated predominantly by heat radiation from the arc column and heat convection from heated gases of the arc flame.

Heat flux intensity diminishes with the increasing distance from the centre of the spot. The distribution of the specific heat flux q_2 cal/cm^2 along the radius of the spot is approximately defined by Gauss probability law (Fig. 1.)

$$q_2(r) = q_{2\,max} e^{-kr^2}, \qquad (2)$$

where

$q_{2\,max}$ - maximum specific heat flux at the spot centre;

k - concentration coefficient of the arc specific heat flux in cm^{-2};

r - distance from the heat source center in cm.

Maximum flux $q_{2\,max}$ rises with the growing amperage, the voltage being constant. When the voltage grows, that is when the arc lengthens, the amperage remaining constant, maximum flux $q_{2\,max}$ drops and the distribution of the specific heat flux becomes less concentrated. Specific heat flux of the submerged electric arc is considerably more concentrated than the heat flux of the open carbon or metal welding arc (Fig.2.). The specific heat flux of gas flame at an equal overall effective power spreads over a substan-

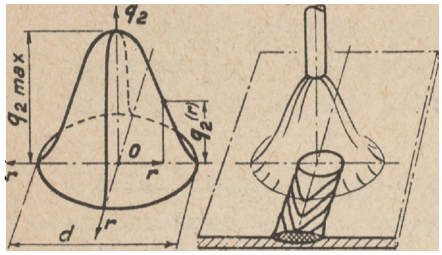

Fig.1. - Scheme of the welding arc heat source;
a - arc cone and flame;
b - arc heat flow distribution (normal circular source).

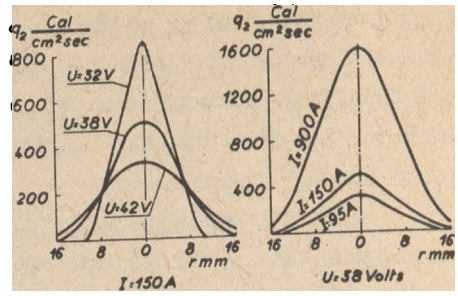

Fig.2. - Effect of current and voltage of the open carbon arc on the distribution of heat flux q_2 over the hot spot.

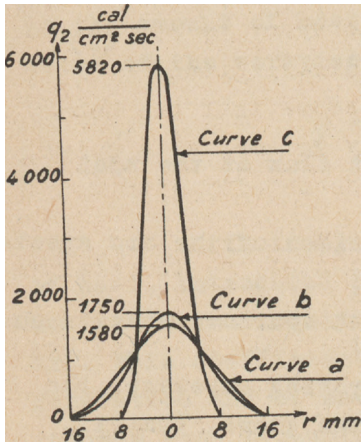

Fig.3. - Distribution of heat flux q_2 over the hot spot of unshielded carbon arc, unshielded metal arc and submerged metal arc (curves a,b and c respectivelly).

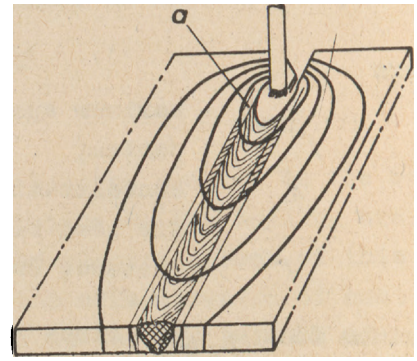

Fig.4. - Scheme of temperature distribution in single arc butt welding of sheets.

tially greater area and is featured by a lower maximum value at the centre of the spot (Fig.3 and 14b).

H e a t f l o w p r o c e s s e s. The heat of a local surface or volume source, concentrated in a comparatively small area of the surface or a small volume of metal, raises the metal temperature to a relatively high value. Heat conductivity of workpiece metal results in a heat flow from the source area and slows down the local heating of metal to the necessary temperature. The process of heat flow in metal may be calculated when characteristics of the heat sources - the effective power and its distribution over the surface or in the volume of a workpiece - are available. Local effect principle of the heat conduction theory shows that the pattern of heat distribution of a local source has a substantial effect upon the temperature field only in the region, adjacent to this source (zone a in Fig.4). Therefore the temperature fields of the workpiece in its region which is far from the welding arc, may be defined with sufficient accuracy by schematizing the pattern of the arc heat flux distribution.

The most simple way is to assume that the heat source is concentrated inan elementary volume: at a point, at a straight line or at a plane, in conformity with the shape of the heat-conductive body.

When more accurate calculation of the temperature is to be carried out for a zone near to the welding arc it is necessary to take into account the real distribution of the specific heat flux over the arc spot, which is approximated by the Gauss law (2) and by the deepening of the arc into the molten pool/6/.

Coefficients of thermo-physical properties for the workpiece metal (their mean values in the rated temperature range) are denoted as follows (see Appendix 2):

λ - thermal conductivity in cal/cm.sec^{o}C;

$c\gamma$ - volumetric heat capacity in cal/cm^3 ^{o}C;

$a = \lambda / c\gamma$ - thermal diffusivity in cm^2/sec.

Surface heat loss from the workpiece to the ambient air is defined by the coefficient α cal/cm^2.sec^{o}C.

In the process of heat flow in arc welding three stages may be distinguished: a) heat saturation process when the temperatures in the field, moving together with the heat source, continue to rise; b) quasi-stationary state when a moving field is practically established; c) levelling of the temperature after arc extinguishing.

B u i l d i n g u p a b e a d upon a massive workpiece is described by the scheme of a constant power point heat source q cal/sec moving uniformly over a straight line over the surface of a semi-infinite conductive body at a speed vcm/sec (fig.5).

The temperature of the quasi-stationary state of the heat flow process in relation to the moving co-ordinates XYZ connected with the source O, is defined by the expression

$$T(R,x)=\frac{q}{2\pi\lambda R}\exp\left[-\frac{v}{2a}(x+R)\right], \qquad (3)$$

where $R^2= X^2+ Y^2+ Z^2$.

The isothermic surfaces of rotation around the axis of source travel are considerably condensed in front of the heat source and rarefied in the region passed by this source.

The calculated temperature grows infinitely with the nearing to the point heat source.

S i n g l e p a s s b u t t a r c w e l d i n g o f s h e e t s is described by the scheme of a linear heat source moving over a longitudinal vertical plane in an infinite plate with a surface heat loss and with a totally levelled temperature across the thickness δ cm. The temperature of the quasi-stationary state of the process in relation to the moving co-ordinates is expressed by

$$T(r,x)=\frac{q}{2\pi\lambda\delta}\exp\left(-\frac{vx}{2a}\right)K_o\left(v\frac{vr}{2a}\right) \qquad (4)$$

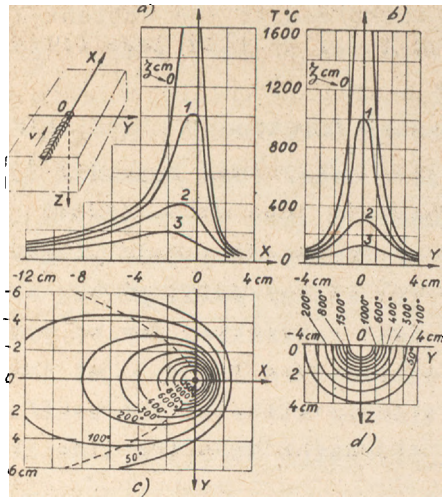

Fig.5. - Spacial temperature distribution (quasi-stationary state) in arc building up of a bead on a steel massive workpiece: q=1000 cal/sec; v=0.1cm/sec. Full lines - isotherms; dash line - curve of maximum temperatures; a - temperature distribution over surface XOY along lines parallel to axis OX; b - temperature distribution over plane YOZ; c and d - isotherms on planes XOY and YOZ.

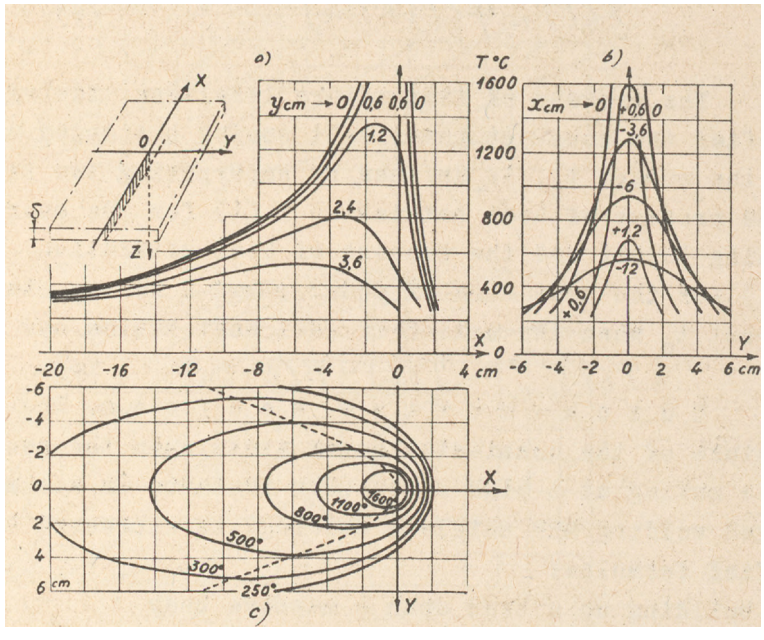

Fig.6. - Plane temperature distribution (quasi-stationary state) in arc butt welding of 10mm thick steel sheets; q=1000 cal/sec; v=0.1 cm/sec; α =0.0014 cal/cm sec °C. Full lines - isotherms; dash line - curve of maximum temperature distribution over surface XOY along lines parallel to axis OX; b - temperature distribution over surface XOY along lines parallel to axis OY; c - isotherms on plane XOY.

where $v^2 = 1 + \frac{\delta \lambda \alpha}{(vc\gamma)^2 \delta}$ - criterion of heat loss effect;

$r^2 = x^2 + y^2$; $K_0(u)$ - Bessel function of imaginary argument of second kind of zero order (see Appendix I).

The heat in the sheet is less concentrated around the arc than in case of the massive body (fig.6).

The temperature T (t) at any point of the moving field during the process of heat saturation may be presented as a product of the temperature T (∞) at the same point in the quasi-stationary state by the coefficient of heat saturation ψ (t), depending upon the time (fig.7).

$$T(t) = \psi(t) T(\infty) \qquad (5)$$

The process of temperature levelling, taking place after the constant power heat source q stopped acting at the moment t_0, is defined by superposing two processes: the process of heat saturation T (t) for the source continuing to act and the process of heat saturation T ($t-t_0$) for the heat sink of equal power-q having started the moment t_0 when the action of real heat source had stopped.

$$T(t)_{t>t_0} = T(t) - T(t-t_0) \qquad (6)$$

Q u i c k - m o v i n g s o u r c e s. The temperature of the quasi-stationary state when the powerful arcs are moving at a high speed (for instance in automatic submerged welding and shielded welding) is expressed by simplifief formulae;

for building up a bead upon a massive body

$$T(t, y_o, z) = \frac{q}{2\pi\lambda vt} \exp\left(-\frac{y_o^2 + z_o^2}{4at}\right) \qquad (7)$$

for butt welding of sheets

$$T(t, y_o) = \frac{q}{v\delta\sqrt{4\pi\lambda c\gamma t}} \exp\left(\frac{2\alpha t}{c\gamma\delta} - \frac{y_o^2}{4at}\right) \qquad (8)$$

where $t = -\frac{x}{v}$ - time elapsed since the arc has intersected plane $Y_0 O Z_0$ on which the point A under examination is located (fig.8).

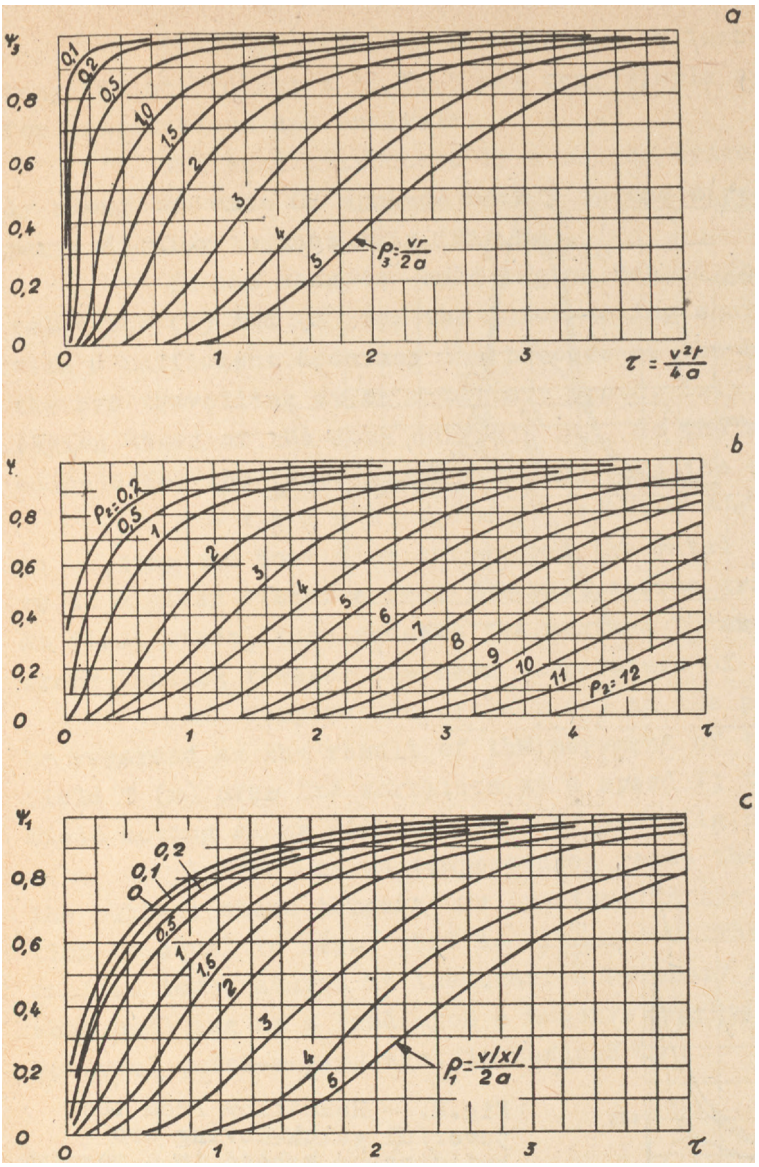

Fig.7. Heat saturation coefficients ψ in relation to the time: a - for point source in semi-infinite body; b - for linear source in a plate with surface heat loss $\left(\rho_2 = \nu \frac{vr}{2a};\quad \tau = \nu^2 \frac{v^2 t}{4a}\right)$;
c - for plane source in a rod with surface heat loss
$\left(\rho_1 = \nu \frac{v|x|}{2a};\ \tau = \nu^2 \frac{v^2 t}{4a}\right)$.

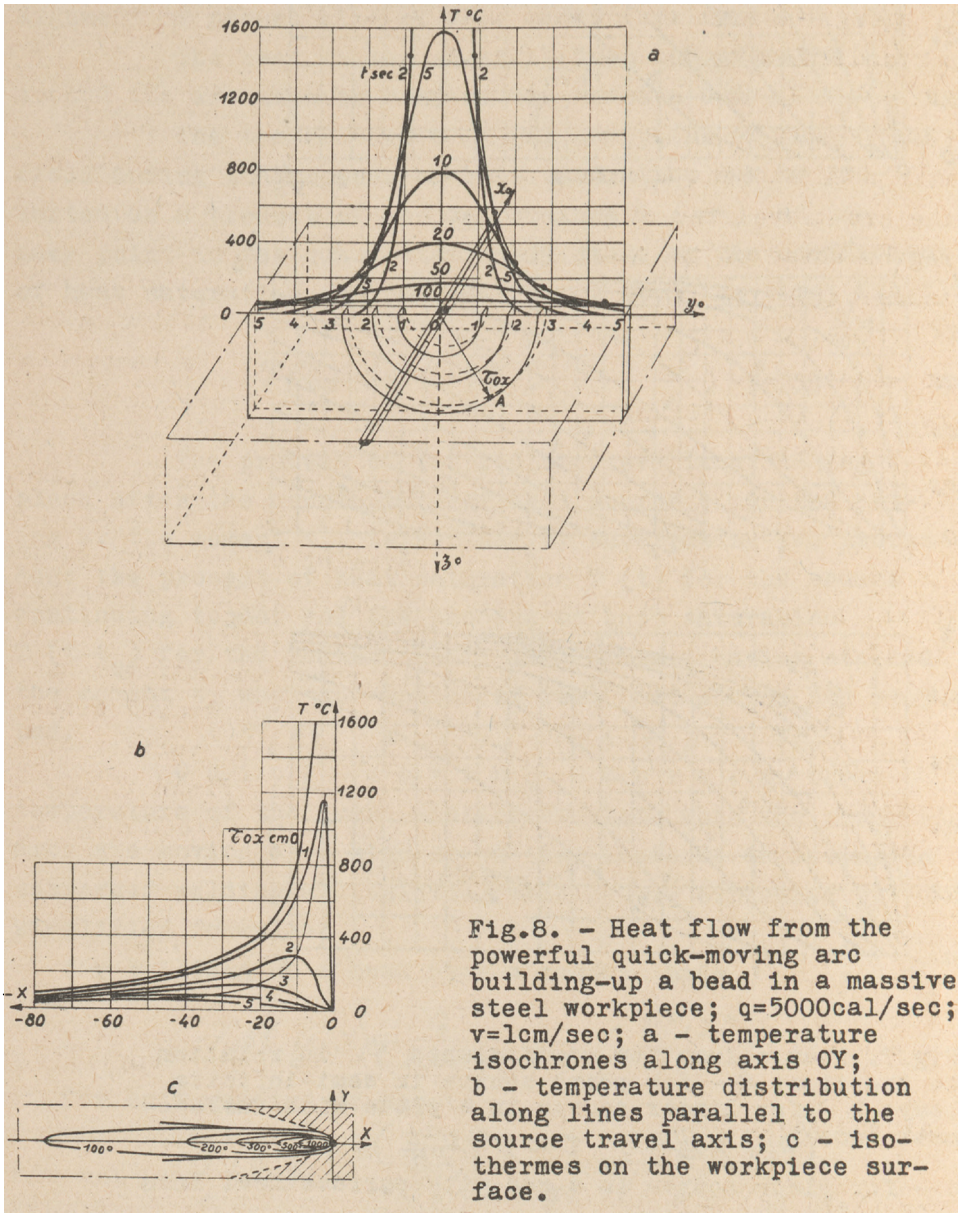

Fig.8. - Heat flow from the powerful quick-moving arc building-up a bead in a massive steel workpiece; q=5000cal/sec; v=1cm/sec; a - temperature isochrones along axis OY; b - temperature distribution along lines parallel to the source travel axis; c - isothermes on the workpiece surface.

These expressions in relation to immovable rectangular co-ordinates X_o, Y_o, Z_o are very simple and convenient for computations and analysis.

The heat introduced by a source travelling quickly along the axis OX spreads mainly in the directions perpendicular to this axis (fig.8a).

In the near-to -weld region behind the arc, the relations (7) and (8) for the quick-moving sources define with a sufficient accuracy the process of the heat flow of the arc travelling at an arbitrary speed. Only in the region ahead of the dash curve in fig. 8c the error in calculating the temperature from the relation (7) exceeds 1%.

M a x i m u m t e m p e r a t u r e s. According to welding arc heat flow throughout the metal the temperature at a given distance from the heat source travel axis at first rises, then reaches the maximum T_m and at last drops tending towards the mean temperature of the workpiece.

The temperature cycle T (t) at the point A may be regarded as the result of the movement of the temperature field T (x) over the workpiece at a speed V; the temperature field moving along with the welding arc (fig.9).

Instantaneous temperatures reach the maximum on the surface where temperature gradient in the travel direction is equal to zero, that is $\frac{dT}{dx} = 0$. The surface of maximum temperatures in the quasi-stationary field (7) when building up a bead upon a massive workpiece by a powerful quick-moving arc, is defined by

$$\frac{r_{ox}^2}{4at_m} = 1 . \qquad (9)$$

where $r_{ox}^2 = y^2 + z^2$;

$t_m = \frac{x_m}{v}$ is the time interval until the temperature at the given point has reached its maximum value.

The maximum temperature surface in quasi-stationary field (8) when thin sheets are butt welded by means of a powerful and quick-moving arc, is expressed by equation

$$\frac{y_o^2}{4at_m} = \frac{1}{2} + \frac{2\alpha}{c\gamma\delta} t. \qquad (10)$$

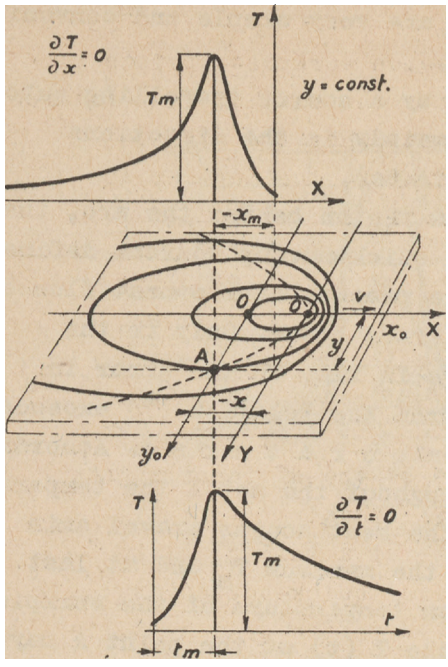

Fig.9. - Temperature variation at immovable point A of a workpiece during welding when temperature field moves with the source.

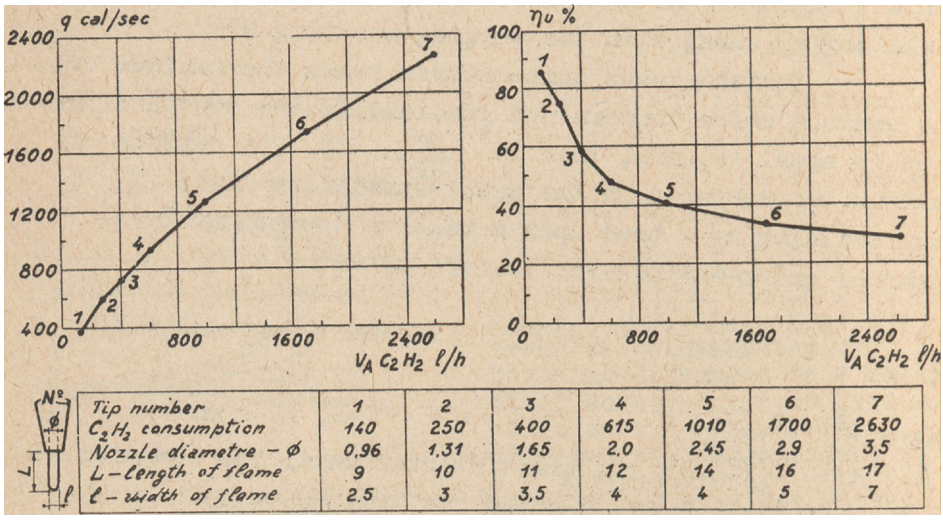

N°	1	2	3	4	5	6	7
Tip number							
C_2H_2 consumption	140	250	400	615	1010	1700	2630
Nozzle diametre - ϕ	0,96	1,31	1,65	2,0	2,45	2,9	3,5
L - length of flame	9	10	11	12	14	16	17
l - width of flame	2,5	3	3,5	4	4	5	7

Fig.10. - Flame effective power, core length (a) and efficiency (b) of metal heating dependent on the acetylene consumption or the tip size of a standard torch.

Maximum temperature surfaces are shown in figure 5,6 and 9 by dash lines.

In the far from weld region workpiece points the heating (cooling) rates as well as the maximum temperatures are the lower and the time instant, when the maximum temperature is attained, is the later, the further the given point is located from the axis of the heat-source travel. The maximum temperature at a point of a massive workpiece in building up a bead by means of a powerful quick-moving arc

$$T_m(r_o) = \frac{1}{e} \frac{q}{v c \gamma \frac{\pi}{2} r_o^2} \qquad (11)$$

is inversely proportional to the square of the distance r_o from the axis of the point-source travel.

The maximum temperature at a thin plate in butt welding with the help of a powerful quick-moving arc at small distances $y_o \ll \sqrt{\frac{\lambda\delta}{\alpha}}$ from the weld axis, is expressed as follows

$$T_m(y_o) = \frac{0{,}484\, q}{v c \gamma \delta 2 y_o} \left(1 - \frac{\alpha y_o^2}{\lambda \delta}\right) \qquad (12)$$

and in case of negligible heat loss, when $\alpha = 0$, is inversely proportional to the distance y_o from the plane of linear source travel.

Both in massive body and in a plate the maximum temperatures T_m are proportional to linear energy q/v of a powerful quick-moving source, that is to the amount of heat introduced by the welding arc to the workpiece per unit of length of a weld or bead.

The effect of finite dimensions of a workpiece, i.e. its thickness, width or length upon the process of welding-arc heat flow may be taken into account by using the so-called method of images, assuming the boundary surfaces impervious to heat. This method provides for the possibility to calculate the temperatures in sheets of medium thickness in bands of medium width, at corners, edges and ribs as well

as in workpieces of complicated configuration limited by a system of orthogonal planes (beams, boxes) /1/,/2/.

Gas Flame Metal Heating

F l a m e t h e r m a l c h a r a c t e r i s t i c s. In order to calculate the process of metal heating with a gas flame it is necessary to know its following main thermal characteristics: the temperature, the effective thermal power q cal/sec, the distribution of flame heat flux q_2 cal/cm^{2}sec. over the hot spot. These characteristics depend upon the net heating value of the combustible gas, the purity of the oxygen and their ratio in the gas mixture.

Gas flame temperature reaches its maximum value on the flame axis close to the core end.

Maximum Temperature of Welding Flame in ^{o}C

Acetylene	3100 - 3200
Methane	1900 - 2100
Butane-propane mixture	2000 - 2100
Coke gas	2000 - 2100
Hydrogen	2100 - 2300

The gas flame heats the metal surface due to the heat exchange processes - forced convection and radiation, intensities of which are growing with the increase in the temperature drop between the flame gases and the metal surface. Hence the effective power of the flame grows with the rise of its temperature and drops with the rise of metal surface temperature.

The effective power q of the flame (its limit value corresponds to quasi-stationary state of metal heating with the moving flame) rises with the increase in the consumption V_A l/hr of the combustion gas (fig.10). Gas flame metal heating efficiency η_{eu} is represented by the ratio of the effective power q of this flame to the total thermal power q_h, which corresponds to the net heating value of the combustive.

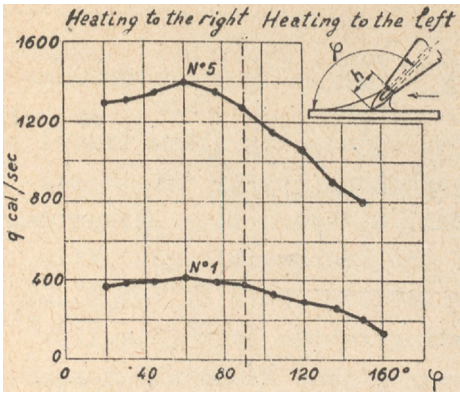

Fig.11. - Standard torch flame effective power in relation to the inclination angle φ of the flame axis to heated metal surface for No. 1 and No. 5 tips.

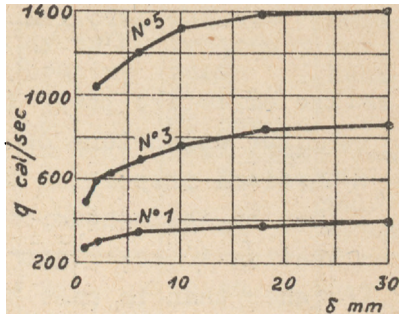

Fig.12. - Standard torch flame effective power(Nos. 1,3 and 5 tips) in relation to heated metal sheet thickness.

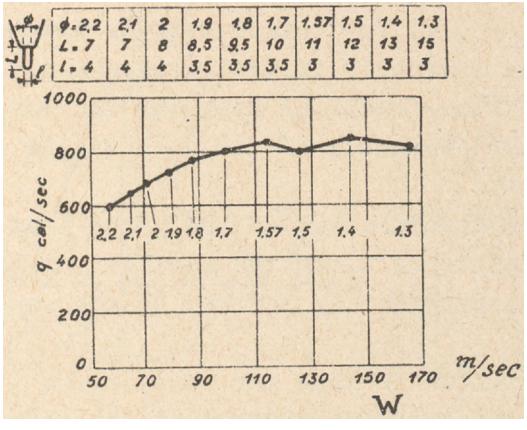

Fig.13. - Standard torch flame effective power and core length in relation to the average rate W of the mixture outflow or to diametre d of the nozzle at a constant acetylene consumption of 400 l/hr (Tip No.3).

For acetylene-oxygen flame, when the net heating value of acetylene equals to 12600 cal/l (at 20°C and 700mmH), this efficiency is as follows:

$$\eta_u = \frac{q}{3,5\ V_A} \qquad (13)$$

The effective power is affected also by flame travel rate, by the dimensions of the workpiece and by the thermophysical properties of metal, although to a lesser degree than by the consumption of the combustible gas. With heating to the right the effective power of the flame is higher than in case of heating to the left (fig.11).

The effective power of the flame rises somewhat with the increase in the flame-travel rate. With the increase in the thickness of the heated metal and in its conductivity the effective power of the flame steps up due to the increase in heat flow into the metal (fig. 12).

The maximum effective power of the flame corresponds to a definite ratio of oxygen and combustible gas. These ratios are somewhat lower than the theoretical ones for the reaction of complete combustion: for acetylene - 2.3, 0.4; for methane - 2.0; for coke gas - 0.8; for hydrogen - 0.4; for butane-propane mixture - 3.5.

The intensity of heat exchange and the effective power of the flame steps up with the increase of average rate of flow W (V=const) of the combustible mixture (fig.13).

The distribution of the flame heat flux q_2 of a conventional torch along the radius r of the metal hot spot may be approximately defined by the realation (2) (fig.14).

In order to ease the calculation it is convenient to characterize the distribution of the flame heat flow by the time constant $t_0=\frac{1}{4ak}$ The concentration coefficient k for a conventional torch flame drops while the time constant t_0 rises with the increase in the tip size and the acetylene consumtion (table 1).

I. Thermal Characteristics of Oxy-acetylene Flame of Standard Torches

Tip size of torch TC-49	Nozzle diametre in mm	Acetylene consumption V_A in ℓ/hr	Flame core length h in mm	Flame effective power q in cal/sec	Efficiency in heating steel η_u in %	Concentration coefficient of the heat flux k in cm^{-2}	Maximum heat flux q_{2max} in cal/cm^2sec	Time const. in heating steel t_o in sec
1	1.0	150	9	380	72	0.39	47	8
2	1.3	250	10	600	68	0.35	67	9
3	1.6	400	11	720	51	0.31	72	10
4	2.0	600	12	920	44	0.28	82	11
5	2.5	1000	14	1270	36	0.23	93	14
6	3.0	1700	16	1750	30	0.20	111	15
7	3.5	2600	17	2250	25	0.17	122	19

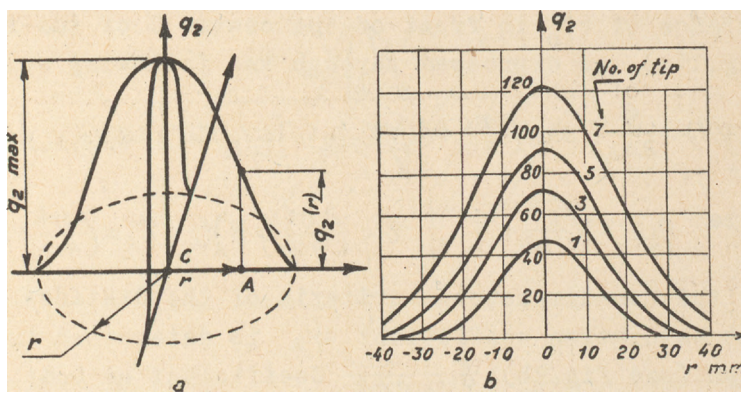

Fig.14. - Heat flux distribution q_2 of the standard torch flame along radius r of hot spot at a 90° inclination angle: a - scheme; b - q_2 distribution at various sizes of tips (various acetylene consumption).

The maximum heat flux q_{2max} along the axis of the acetylene-oxygene flame of a conventional torch is by 8-12 times less than the flux q_{2max} of an open welding arc having approximately the same effective power. Therefore gas flame heats up the metal considerably more slowly and smoothly than the welding arc.

Multi-flame and slot type torches allow to adjust the shape and dimensions of the flame as well as to distribute the heat flux after a pre-set pattern over the required areas of the metal surface to be heated. Such torches are used in gas-press welding as well as in surface flame-hardening of metals.

H e a t i n g o f t h i n s h e e t s (with complete levelling of the temperature across the thickness) by a conventional torch flame with the axis perpendicular to the sheet surface, which is either stationary or moving along the straight line at a constant speed of vcm/sec, may be defined by the scheme of a moving normal-circular heat source in a thin plate with heat loss. The temperature during the process of heat saturation in relation to the movable system of co-ordinated XYZ, with its centre located at the imaginary concentrated source q travelling at a distance of vt_0 in front of the centre C of the real source (fig.15a), is expressed through the following equation

$$T(x,y,t)=\frac{q}{2\pi\lambda\delta}\exp\left(-\frac{vx}{2a}+\beta t_0\right)K_0(\rho_2)\times\left[\psi_2(\rho_2,\tau+\tau_0)-\psi_2(\rho_2,\tau_0)\right] \quad (14)$$

where $\rho_2=r\sqrt{\frac{v^2}{4a^2}+\frac{\beta}{a}}$; $\tau=\left(\frac{v^2}{4a}+\beta\right)t$; $\tau_0=\left(\frac{v^2}{4a}+\beta\right)t_0$,

are the non-dimensional criteria of the distance and time; heat saturation coefficient ψ_2 is determined from the graph (see fig.7b); $\beta=\frac{2\alpha}{c\gamma\delta}$ Coefficient of heat exchange α cal/cm^{2}sec is to be chosen as a mean value from the coefficients of heat exchange between the flame and the upper heated surface of the sheet (α_n =0.01-0.015cal/cm^{2}sec^{0}C) and between the lower free surface of the sheet and the calm air, α_c = 0.001cal/cm^{2}sec^{0}C).

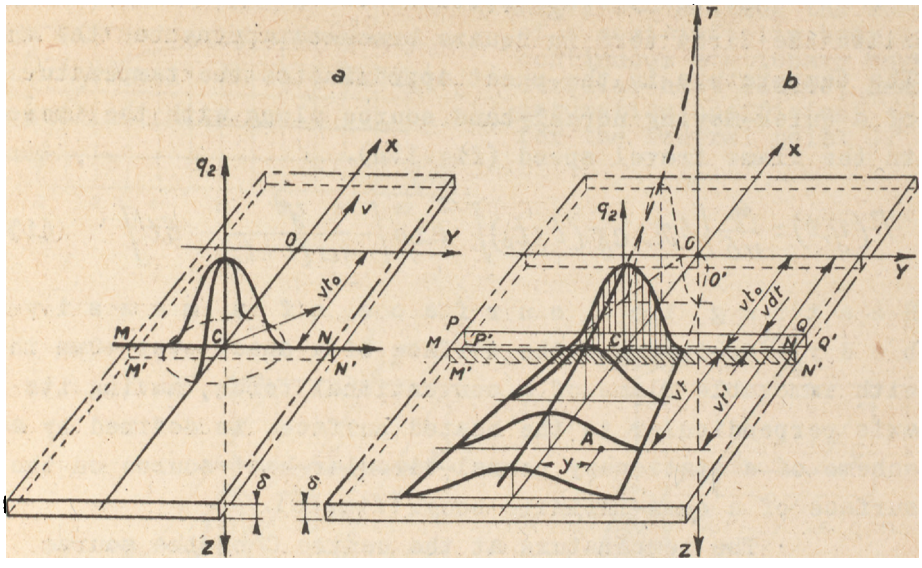

Fig.15. - Scheme of heating a thin sheet: a - by a superficial normal-circular heat source; b - by a quick-moving superficial normal-linear heat source.

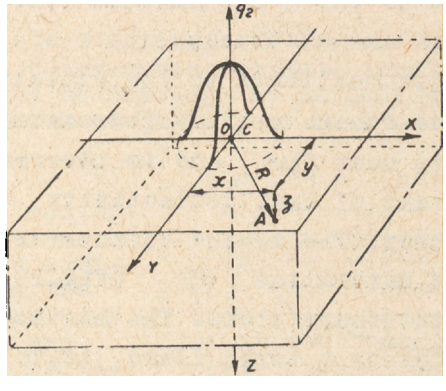

Fig.16. - Scheme of heating a semi-infinite body by a superficial normal-circular heat source.

As the process approximates its quasi-stationary state the first term in square brackets approaches the unit. The temperature in the sheet approximates the temperature of a quick-moving normal-band source along with the increase in the flame travel speed (fig.15b).

$$T(y,t)=\frac{q}{v\delta}\left[4\pi\lambda c\gamma(t+t_o)\right]^{-1/2}\exp\left[-\frac{y^2}{4a(t+t_o)}-\beta t\right]. \quad (15)$$

Heating the surface of a massive body (for instance the surface of a sheet over 40mm thick) with immovable flame of a conventional torch, having its axis perpendicular to the heated surface, is defined by a scheme of a stationary normal-circular heat source on the surface of a semi-infinite body. (fig.16).

The temperature at the centre C of the source during the process of heat saturation, being apparently the maximum temperature of the heated body, is expressed by the following formula

$$T(t)=\frac{q}{2\lambda\sqrt{4\pi a t_o}}\cdot\frac{2}{\pi}\,arctg\sqrt{\frac{t}{t_o}}. \quad (16)$$

The first cofactor shows the maximum temperature at the central point in the stationary state of the process. This temperature is proportional to the effective power q of the flame and to the square root of the concentration coefficient k of its heat flux, and is inversely proportional to the coefficient of heat conductivity λ for the material of the heated body. The second cofactor represents the coefficient of heat saturation ψ (fig.17) which tends to unity in the stationary state. The heating of the surface of a massive body by a torch flame, travelling at a great speed, is defined by the expression for the temperature of the quick-moving normal-linear source (fig.18)

$$T(y,z,t)=\frac{q}{2\pi v\lambda\sqrt{t(t_o+t)}}\exp\left[-\frac{z^2}{4at}-\frac{y^2}{4a(t_o+t)}\right] \quad (17)$$

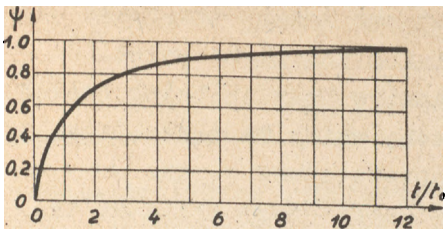

Fig.17. – Heating the surface of a semi-infinite body by a continuous stationary normal-circular heat source; heat saturation coefficient ψ for the central point C.

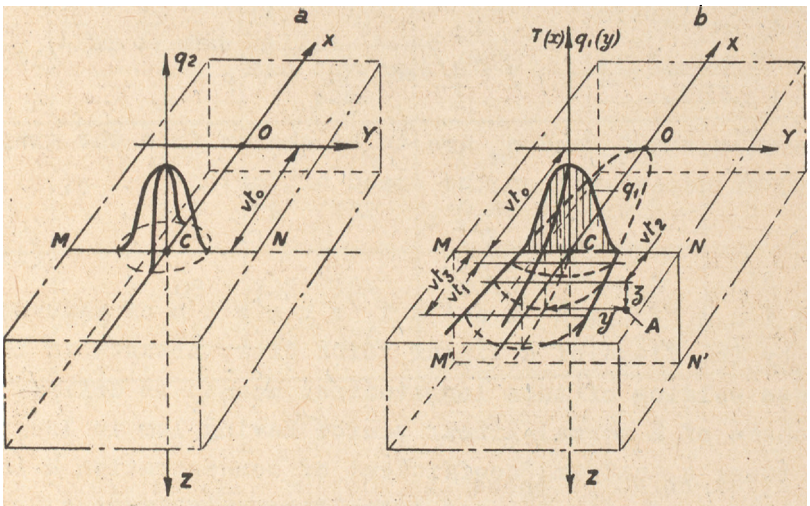

Fig.18. – Scheme (a) of heating the surface of a semi-infinite body by a powerful quick-moving normal-circular heat source $q_2(r)$ and scheme (b) of heating the surface of a semi-infinite body by a normal quick-moving linear heat source $q_1(y)$

Fig.19. – Relative maximum temperature t_m for the surface points of a semi-infinite body along the axis of a normal-circular heat-source travel and coefficient n_m for defining the distances between the points with maximum temperature points and heat source centre in relation to criterion ρ.

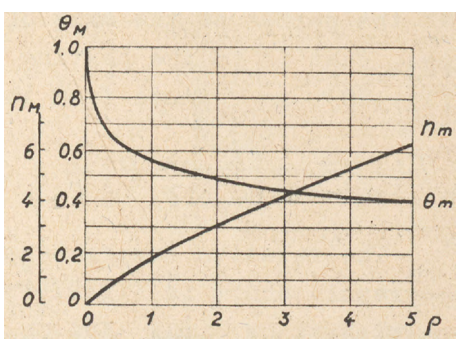

where time t is to be recorded from the moment the flame centre intersects the plane containing the given point.

When the surface of a massive body is being heated by the flame of a conventional torch, which is travelling along the straight line at the constant speed v_J the maximum temperature T_m of the quasi-stationary state at the point M of the axis of the flame travel and the distance f of the point M from the centre C of the flame are defined as follows:

$$T_m = \frac{q}{2\lambda\sqrt{4\pi a t_o}}\,\theta_m\,, \qquad f = \sqrt{4 a t_o n_m} - v t_o \tag{18}$$

The coefficients θ_m and n_m are to be chosen from the graph (fig.19) in dependence on the speed criterion

$$\rho = \frac{v t_o^2}{4a} \tag{19}$$

H e a t i n g t h i n m e t a l s h e e t s of thickness δ cm by the flame of a linear torch (for instance in the gas-press welding of tube longitudinal seams) is defined by a scheme of a normal-linear source having lcm in length, linear power q_1 cal/cm, coefficient of concentration k in the direction of axis OY, and travelling quickly at a constant speed of vcm/sec in the direction OX of the flame axis (fig.20). The heat exchange coefficient between the flame and the metal is equal to α_n . The sheet temperature T (t) at the points of the axis of the torch travel under the flame, that is in the heating stage $t < \frac{l}{v}$ (region II in fig. 20), is defined from the following relation

$$T(t) = \frac{q_1}{2\sqrt{\alpha_n \lambda \delta}}\,\theta\left(\frac{t}{t_o};\ \tau_o\right) \tag{20}$$

The relative temperature θ is to be chosen from the nomographic chart in fig.21 in dependence on relative duration of heating $\frac{t}{t_o}$ and on non-dimensional criterion $\tau_o = \frac{2\alpha t_o}{c\gamma\delta}$ Thermal characteristics of the flame for some types of the linear multi-flame torches are given in table 2.

The sheet temperature T(t) at the points of the

2. Characteristics of the Heat Flux Distribution for the Flame of Linear Torches and Effectiveness of the Heating Process for 1.5mm Thickness Steel Sheets

Nozzle diametre in mm	Nozzle gap δ in mm	Acetylene consumption per nozzle V_A' in ℓ/hr	Acetylene consumption per unit of length V_A in ℓ/cm hr	Effective power per nozzle q' in cal/sec	Effective power per (unit length) q_1 cal/cm sec	Heat flux concentration coefficient $k = \frac{1}{4at_o}$	Time constant in heating of steel t_o in sec	Maximum flame heat flux in cal/cm^{2}sec	Flame heat exchange coefficient α_n in cal/cm^{2}sec$^\circ$C
0.75	4	75	188	71	178	0.48	6.5	70	0.011
	6		125	79	132	0.89	3.5		0.015
1.0	8	150	188	132	164	0.39	8.0	58	0.011
	12		125	151	126	-	-	-	-

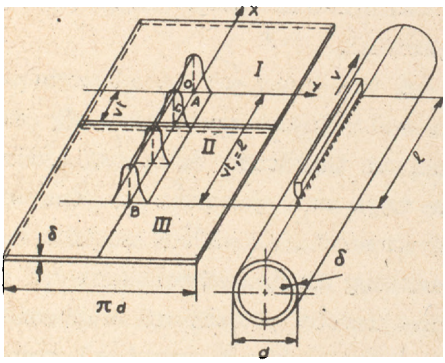

Fig.20. - Scheme of heating the longitudinal weld of thin-sheet tube by the flame of a quick-moving linear torch of length ℓ

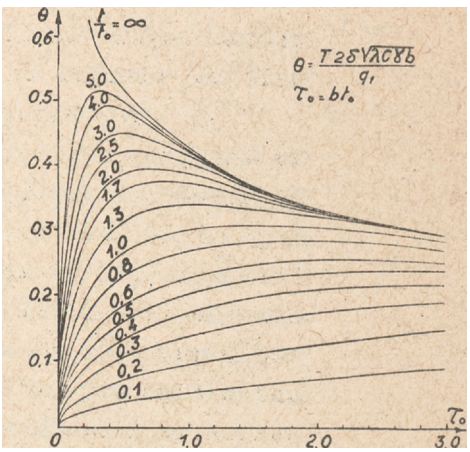

Fig.21. - Relative temperature at the points at axis OX as function of dimensionless time τ_o and criterion t/t_o in the heating of thin sheet by a quick-moving linear torch flame.

torch axis travel behind the flame (fig.20, region 3) that is in the cooling stage $t > \frac{\ell}{v}$ is determined as the difference of temperatures (20)

$$T_1(t) = T(t) - T\left(t - \frac{\ell}{v}\right) \cdot \qquad (21)$$

Examples of such calculation are given in the literature /2/,/3/,/5/.

THERMO-CYCLE IN SEAM ARC WELDING AND BEAD BUILDING UP

The thermo-cycle, that is the alteration of temperature during welding at a given point of the weld or in the zone adjacent to this weld, is the basis for evaluating the heat effect of the welding process upon the structural changes in the base of weld metals. The parameters of the welding process conditions might often be selected in such a way which by meeting the requirements of welding productivity and shaping of the weld joint provides for a thermal cycle involving favourable structural changes as well as changes of properties.

The structure of the heat affected zone as well as the properties of the weld joint must satisfy various requirements which depend on the kind of metal, the technology of manufacture, the type and purpose of the weldment. For instance, in welding structural alloy steels a considerable time lapse of heating at a temperature of over 900°C may lead to an undesirable growth of austenite grains and a high rate of cooling in the sub-critical range of austenite transformation may cause an increase in the hardness as a consequence of quenching.

By calculating the thermal cycle it is possible to establish the limits of welding technological conditions which do not involve a local change in plastic properties. This change can diminish the supporting power of the weldment, particularly by impact loads, in the presence of

stress concentrators and low working temperatures.

S i n g l e p a s s w e l d i n g. The main parameters of the thermal cycle in the heat affected zone adjoining the weld in the single-pass seam welding or bead building up are the following: the maximum temperature T_{max}, the instantaneous rate of cooling w °C/sec at a given temperature T, and the heating time t_h above a given temperature T (fig.22).

In the arc building-up a bead on a massive workpiece (see fig.5 and 23a) the instantaneous rate of cooling at a given temperature is found from the following expression

$$w = \frac{2\pi\lambda (T-T_0)^2}{q/v}, \qquad (22)$$

where T_0 - initial temperature of the workpiece or the temperature in simultaneous pre-heating. In the single-pass butt welding of sheets or in the building up a bead on a sheet of small thickness (see fig.6 and 23b) the instantaneous rate of cooling is found from this relation:

$$w = \frac{2\pi\lambda c\gamma (T-T_0)^3}{(q/v\delta)^2}. \qquad (23)$$

In the building up a bead on a sheet of any thickness (fig.23b) the cooling rate is taken from the nomographic charts (fig.24a and b). When determining the cooling rate with the help of the nomographic charts or the expressions (22) and (23), in place of the true values of the linear energy q/v and the metal thickness δ their reduced values are taken which had been obtained in multiplying q/v and δ by coefficients taking into consideration the effect of the weldment shape (table 3).

The time lapse t_h of the heating over a given temperature in the building up a bead on a massive workpiece

$$t_h = f_3 \frac{q/v}{\lambda (T_m - T_0)}, \qquad (24)$$

is proportional to the linear energy q/v of the arc. In the single pass butt welding of sheets this duration

$$t_h = f_2 \frac{\left(q/v\delta\right)^2}{\lambda c \gamma \left(T_m - T_o\right)^2} \qquad (25)$$

is proportional to the square of the arc specific energy $\frac{q}{v\delta}$ In these formulae - T_m is the maximum temperature of the cycle (see fig.22) and the coefficients f_3 and f_2 are to be chosen in accordance with the non-dimensional temperature $\Theta = \frac{T - T_o}{T_m - T_o}$ which varies within the range from 0 to 1 in the nomographic chart in fig. 25.

M u l t i - l a y e r w e l d i n g. In the multi-layer welding by long sections each previous layer has enough time for cooling before the next one is to be brought on. That is why the thermal cycle of any layer is practically independent of previous ones. However the smoothened temperature by welding subsequent layers may affect the structure of the weld or the adjacent zone. For instance, such an effect can temper a previously hardened structure (fig.26).

In welded steels, susceptible to hardening and cold cracking it is necessary to check up the cooling conditions of the first layer in heat affected zone of which in case of fast cooling and sharp hardening cracks may appear. Cooling rate w of the first layer in a multi-layer weld is determined from the expression (22) and the nomographic charts (fig.24) for building up a bead on the sheet.

Different conditions of heat loss are taken into account by using in the calculation instead of true values of the thickness of welded sheets and linear energy $\frac{q}{v}$ their reduced values given in fig. 27.

The cooling rate may be lowered by increasing the linear energy, that is the cross-section of the layer, and by rising the pre-heating temperature of the workpiece.

In multi-layer welding by short sections the thermal effects of subsequently welded layers are summed up, thus contributing to the slow-down of the cooling for

3. Reduction Coefficients

Value to be reduced	First layer of the butt weld; bevelling angle 60^0	Building up single pass butt welding	First layer in tee welding or lap welding
q/v	3/2	1	2/3
δ			1

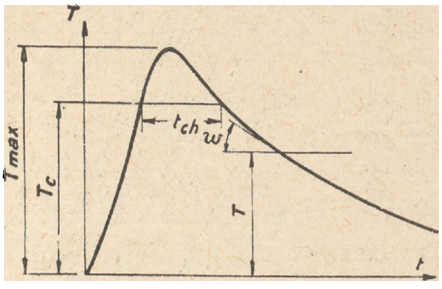

Fig.22. - Scheme of thermal cycle for heat affected zone adjoining the weld in the single-pass welding or in the building up of a bead.

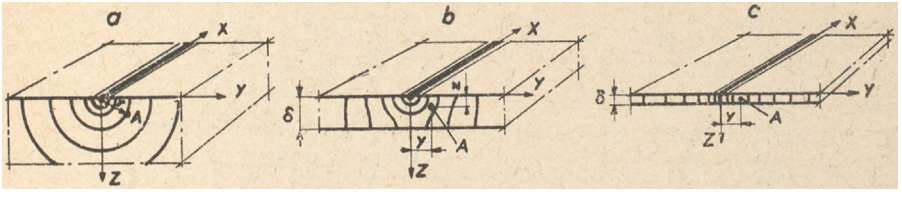

Fig.23. - Schemes of heat flow from a moving point source on the surface: a) - of a massive body, b) - of a thick plate, c) - of a thin plate.

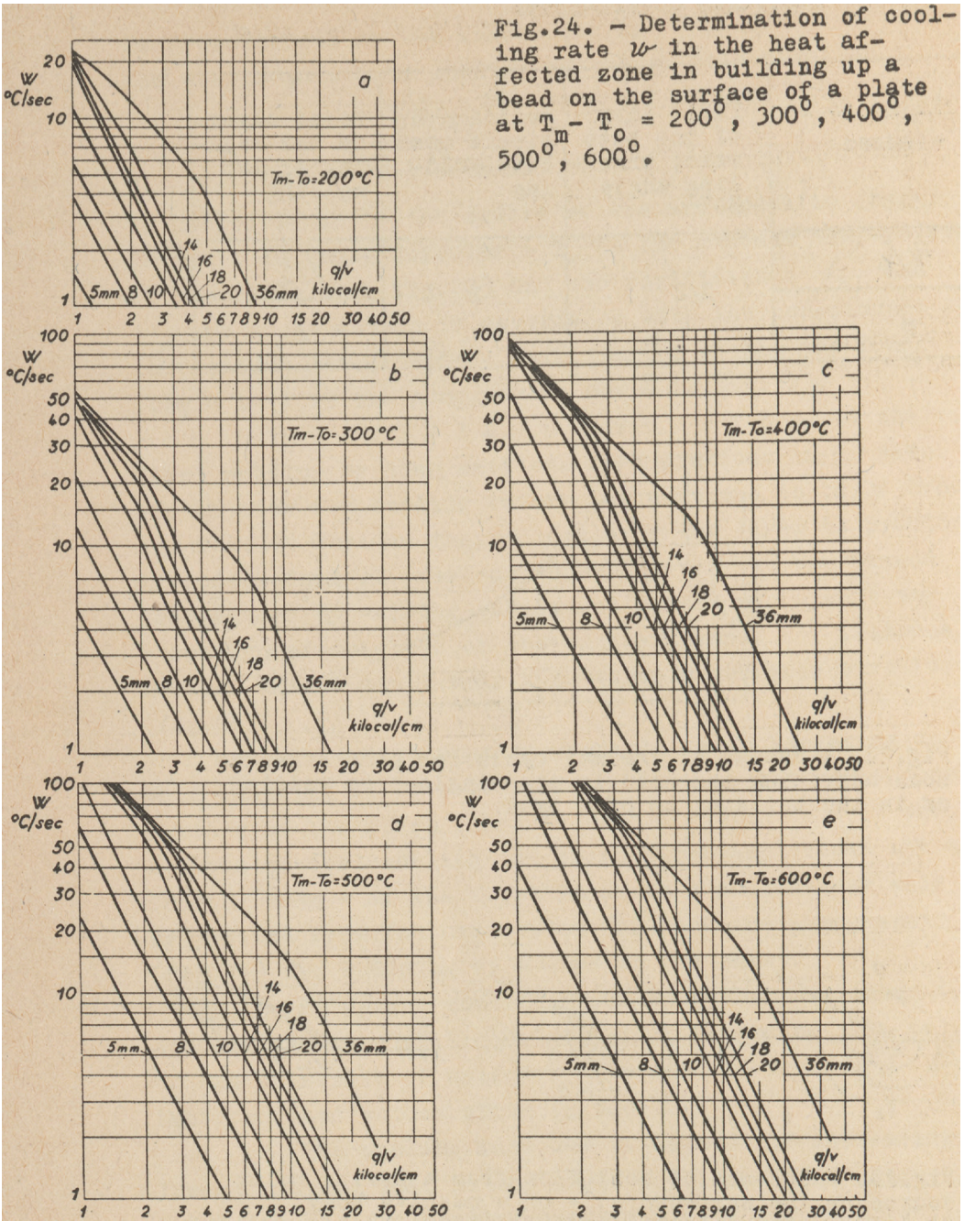

Fig.24. – Determination of cooling rate w in the heat affected zone in building up a bead on the surface of a plate at $T_m - T_o = 200^o$, 300^o, 400^o, 500^o, 600^o.

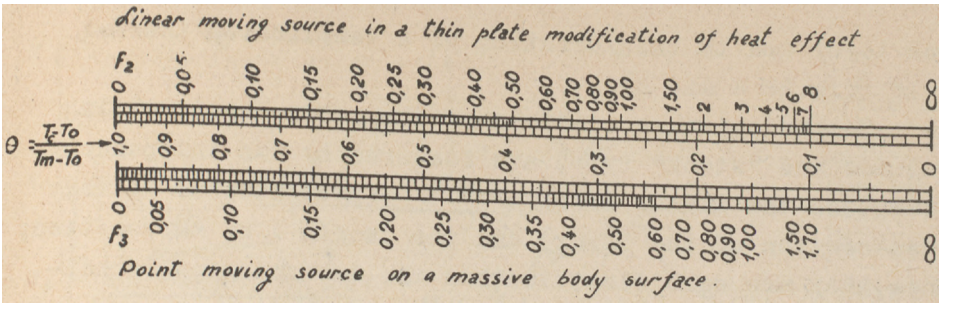

Fig.25. - Determination of over-heat time t_4 above given temperature T: in building a bead on a massive body; in single-pass butt welding of sheets.

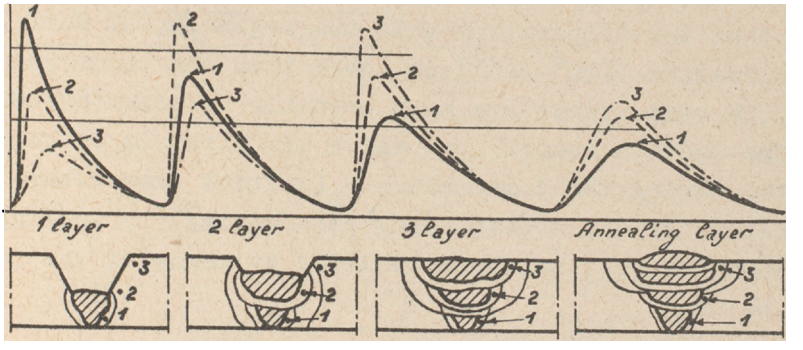

Fig.26. - Multi-layer welding by long sections: thermal cycle (a) and modification of heat effect (b).

Coefficients correctifs	a	b	c	d	e
q/v	1	$3/2$	$2/3$	$2/3$	$1/2$
δ	1	$3/2$	1	1	1

Fig.27. - Corrective coefficients of thickness and linear energy for cooling rate calculation of the first pass of a multi-layer weld,a) building up a bead on a plate;b) butt welding, V - bevelling;c) lap welding; d) tee welding (second weld); e) cross welding (foufth weld).

each layer and to the formation of a complicated thermal cycle (fig.28 a and b).

Technological conditions of the multi-layer welding (cascade and "stack" type) are featured by two independent parameters-the linear energy q/v (proportional to the cross-section of the layer) and the length l of the section; hence they are more flexible than the technological conditions for the single-pass welding.

The length of the section is chosen on the basis of the following considerations:the temperature T_b in the heat affected zone of the first layer ,- at the moment when the heat wave from next layer is to be imposed ,-should not drop lower than the temperature M at the beginning of martensite transformation (200^0-300^0),or lower than the temperature at which the cold cracks are most probable to occur(60-200^0C).

The section length l at which the first layer built up on metal having the temperature T_0(initial temperature or temperature of the accompanying pre-heating) is cooling down to temperature T_b, may be calculated by means of the formula given below

$$\ell = \frac{0,7\, k_3\, k_2\, q^2}{\delta^2 v (T_b - T_0)^2} \qquad (26)$$

where q - effective power of the arc in welding the first layer cal/sec; v - travel rate of the arc, cm/sec; k_2 - coefficient of arc net burning time assumed to be equal to unit for the automatic multi-arc welding and to 0.6 - 0.8 for the manual multi-layer welding; k_3 - correction factor, assumed to be equal to 1.5 for butt joints, 0.9 for tee joints and 0.8 for cross joints. The temperature T_b in the cooling of the first layer is the higher the more heat is introduced to this layer. This temperature increases with the rise of the arc linear energy and the initial temperature T_0 of the metal under welding, as well as with the decrease in the length l of the layer section and the time interval between welding subsequent layers.

Conditions for the multi-layer welding by short sections may be selected in such a may as to make the weld and zone near to it remain in the lower subcritical range -

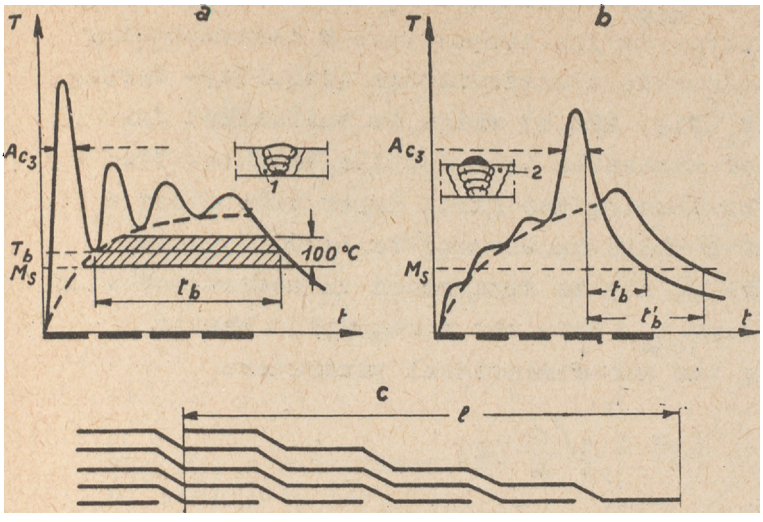

Fig.28 - Thermal cycle in the heat affected zone in multi-layer welding by short sections;a - first layer (point 1); b - last layer (point 2); c - scheme of cascade welding.

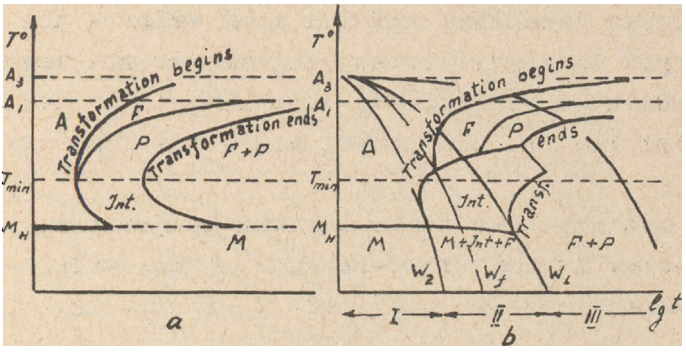

Fig.29. - Diagrams of austenite transformation; a - isothermic transformation; b - continuous cooling transformation; W_1 - cooling rate corresponding to the beginning of martensite formation; W_2 - cooling rate of 100% martensite formation; I - zone of complete hardening; II - zone of stable structures; W_f - cooling rate at which ferrite separation begins. A - austenite; F - ferrite; P - perlite; Int.- intermediate structures(bainite); M- martensite.

from the temperature T_{min}, corresponding to the minimum stability of austenite, to the temperature M corresponding to the start of martensite transformation (fig.29a)- during the time interval t_b(fig. 28a,b) which is sufficient for the decomposition of austenite into ductile bainite. The time interval t_b for heating the first layer zone above a certain temperature T which is assumed to be 50°C higher than the temperature M, may be determined in accordance with the total welding time t_c, from the nomographic charts (fig.30) connecting the non-dimensional parameters

$$\beta t_e \; ; \; \beta t_c \; ; \; \rho_1 = \sqrt{\frac{a}{\beta}}\,|x|$$

and

$$\Theta = \frac{2\lambda\delta\beta}{k_1 k_2 q}\sqrt{\frac{a}{\beta}}\,(T-T_o)$$

where $\beta = \frac{2\alpha}{c\gamma\delta}$ sec^{-1} - coefficient of temperature loss /x/ - rated distance of the heat affected zone from the centre of the source, being equal: for butt welds - the half width of the upper bevelling and for bead welds - the half of the weld leg; k_2 - coefficient of the arc net burning time; k_1 - reduction coefficient equalling to 1 for butt joint, 0.67 -for tee and lap joints and 0.6 - for cross joints.

The heating time above a given temperature is the longer the greater is the cross-section of the weld, - i.e. the sheet thickness and the angle of V of the edges.

FILLER METAL MELTING IN ARC WELDING

The welding arc melts the electrode which is pre-heated by the current over a section from the current supply to the arc.

R o d e l e c t r o d e s. The heating of a rod electrode is determined by heat generation in the metal core according to the Lenz-Joule low and by heat loss through the rod lateral surface.

The temperature T(t)°C of a steel rod electrode of the diametre d, mm and heated by the current Ia from the

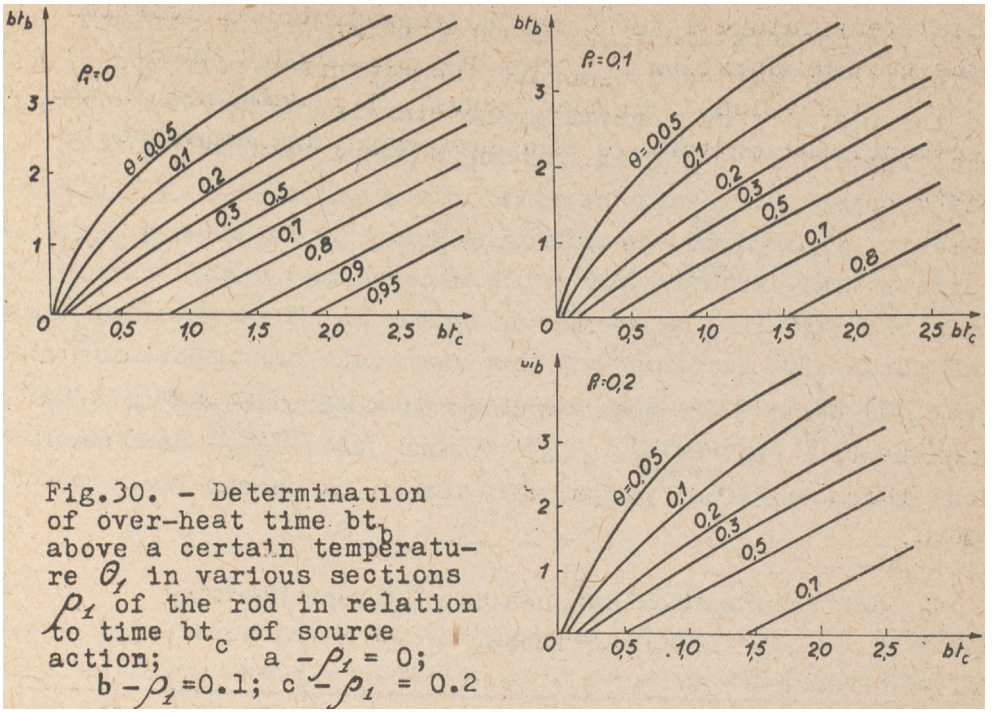

Fig.30. – Determination of over-heat time bt_b above a certain temperature θ_1 in various sections ρ_1 of the rod in relation to time bt_c of source action; a – ρ_1 = 0; b – ρ_1 =0.1; c – ρ_1 = 0.2

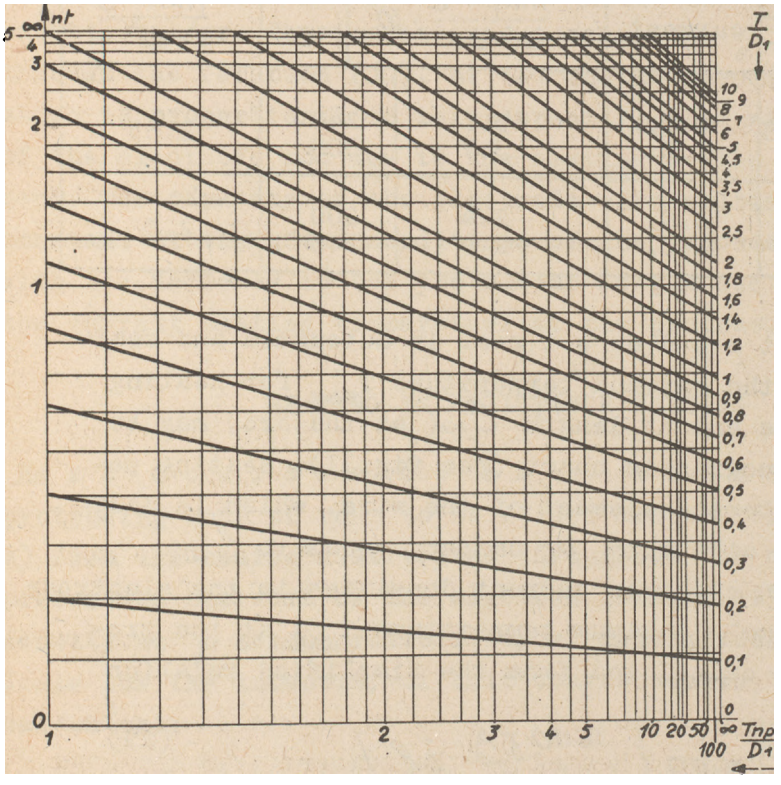

Fig.31. – Calculation of electric current heating process in a mild – steel wire electrode.

initial temperature $T_0 = 0^{\circ}C$ may be represented in relation to the heating duration t_{sec} by the nomograph (fig.31).

The values n in sec^{-1} and $T_{np}\,^{\circ}C$, contained in the non-dimensional criteria of the nomograph, are expressed as follows

$$n = \frac{A}{m d_1^2}\left(\frac{T_{np}}{D_1} + 1\right) \qquad (27)$$

$$T_{np} = m d_1 j^2 \qquad (28)$$

where $j = \frac{I}{\pi d_1^2/4}$ - current density in electrode rod in a/mm^2

Coefficients $A\ \frac{mm^4\,^{\circ}C}{a^2\,sec}$, $D_1\ ^{\circ}C$ and $m\ \frac{mm^3\,^{\circ}C}{a^2}$ dependent on the thermo-physical properties are to be chosen from the table 4.

4. Coefficients for Calculating Current Heating of Electrodes

Type of electrode		Type of current	A $\frac{mm^4\,^{\circ}C}{a^2\,sec}\cdot 10^{-2}$	D_1 $^{\circ}C$	m $\frac{mm^3\,^{\circ}C}{a^2}$
Wire	Coating				
Mild steel	Stabilyzing	D.C. A.C.	3.1 3.7	240 300	2.65
	OMM-5 UONI-13	D.C. A.C.	2.4 2.7	200 240	2.5

E l e c t r o d e w i r e. In automatic and semi-automatic welding the maximum temperature T_{max} for heating the protrusion wire end of length ℓ_{cm} (at the arc) may be determined from nomographic chart (see fig.31). Heating period t for each material element of the wire, which is delivered into the arc at a rate w cm/sec, equals to ℓ / w.

With high electric current densities in the electrode wire $j > 40$-$50\ a/mm^2$ - maximum temperature T_{max} at the protrusion end may be calculated from the simplified relation below

$$T_{max} = (D_1 - T_0)\exp\left[\frac{3600\gamma A}{\alpha_t \rho D_1} j^2 \ell\right] \qquad (29)$$

where $j = \frac{I}{\pi d_1^2/4}$ - density of electric current, a/mm^2;
α_{melt} - coefficient, gr/a.hr
T_o - wire initial temperature, °C;
γ - wire metal density, gr/cm^3.

M e l t i n g o f e l e c t r o d e s. Electrode rod or wire metal pre-heated by current to the temperature T_m, is next heated, melted and overheated by the electric arc to an average temperature T_k of molten drops which fall off the end of the electrode. The electrode melting capacity g_p in gr/sec and the melting rate w in cm/sec are connected with the total electric power UI of the arc through the following formula:

$$g_p = w\gamma \frac{\pi}{4} d^2 \frac{0{,}24\eta_e UI}{S_k - S_m} \qquad (30)$$

where η_e - efficiency of the process of heating the electrode by the arc; S_k and S_m - heat contents of bare electrode metal at the temperatures T_k and T_m or heat contents of the metal and the coating layer taken for the unit of the core weight, cal/gr. The instantaneous capacity g_p expressed through the relation (30), or the instantaneous melting rate, which is proportional to this capacity, rise with the melting of the electrode rod due to the heating by the electric current. The capacity of the electrode-wire melting rate remains constant at the given conditions of the process and grows with the increase in the protrusion length due to the rise of the current heating temperature at the protrusion end.

HEATING IN RESISTANCE WELDING

H e a t s o u r c e s i n b u t t w e l d i n g. The protruding ends of rods to be welded are heated:
a) from the source distributed throughout the metal and representing the work of the electric current with j a/cm^2 density at ρ ohm/cm resistivity of metal; according to Lenz-Joule low the intensity of this source equals to $w = 0.24\rho j^2$ cal/cm^{3}sec;

b) from the concentrated heat source having q_2 cal/cm^{2}sec specific power, generated at the contact surfaces of F cm^2 cross-section and representing the work of jF electric current at Kohm contact resistance (in resistance welding) or at R resistance of the gap between the end-faces (in flash welding) $q_2 = 0{,}24\,\kappa j^2 F$.

T h e r e s i s t i v i t y o f m e t a l s increases with the temperature rise, the increase being particularly sharp in ferromagnetic metals (iron and steel in α phase (fig.32). In calculating the electric current heating within a broad temperature range it is necessary to take into account the temperature dependence of the ratio of the resistivity ρ to the volumetric heat capacity $c\gamma$.

This dependence may be approximately defined through the following linear relation

$$\frac{\rho}{c\gamma} = \frac{\rho_o}{(c\gamma)_o}\left(1+\beta T\right) \qquad (31)$$

The rated values for the ratio $\frac{\rho_o}{(c\gamma)_o}$ at zero temperature and for the temperature coefficient β are given in table 5.

I n r e s i s t a n c e b u t t w e l d i n g of rods the power q_2 of the contact source, representing the work of electric current concentrated close to the region of the end faces at the local contact areas, decreases rapidly at the early stage of the process. That is why for calculating the heating temperature at the late stage of the process the additional contact source is assumed to be instantaneous, applied at the moment of current switching in (t=0) and having the following specific energy

$$Q_2 = \frac{\mu\sqrt{\lambda c\gamma}}{\beta j\sqrt{0{,}24\frac{\rho_o}{(c\gamma)_o}}}\,\frac{\kappa}{j} \quad cal/cm^2 \qquad (32)$$

where k and μ - rated coefficients dependent on the properties of the rod metal and on the pressure (see table 5). Smaller values of the coefficients correspond to higher pressures.

5. Coefficients for Calculating the Heating of Rods in Resistance Butt Welding

MATERIAL	$\frac{\rho_o}{(c\gamma)_o}$ ohm.cm⁴°C/cal	β 1/°C	μ	τ	j^2t a²sec	k cal a/cm⁴
Mild steel 10 (0.1%C)	15×10^{-6}	3.8×10^{-3}	2.6–3	1.27–1.21	/93–89/$\times10^6$	/0.19–0.24/$\times10^6$
Steel 45 (0.45%C)	22×10^{-6}	3.0×10^{-3}	2.0–2.3	1.18–1.14	/75–72/$\times10^6$	/0.17–0.21/$\times10^6$
Steel 25H3 (0.25%C; 3%Ni)	23.5×10^{-6}	2.23×10^{-3}	1.6–1.8	0.98–0.94	/78–75/$\times10^6$	/0.21–0.25/$\times10^6$
Tool steel (0.1%C; 0.58%Mn) 12.2%Cr	35×10^{-6}	1.36×10^{-3}	0.9–0.95	0.76–0.74	/67–65/$\times10^6$	/0.20–0.23/$\times10^6$
Steel P18 (0.71%C; 4.26%Cr; 1.07%V; 18.45%W)	50×10^{-6}	0.64×10^{-3}	0.32–0.34	0.95	124–10^6	/0.18–0.22/$\times10^6$
Stainless steel 18–8	72×10^{-6}	0.28×10^{-3}	0.07–0.08	0.30	62–10^6	/0.09–0.12/$\times10^6$
Aluminium	5.65×10^{-6}	2.33×10^{-3}	0.34–0.36	0.8	250–10^6	/0.17–0.18/$\times10^6$
Copper	2.2×10^{-6}	2.8×10^{-3}	0.14–0.15	1.3–1.25	/880–850/$\times10^6$	/0.12–0.13/$\times10^6$

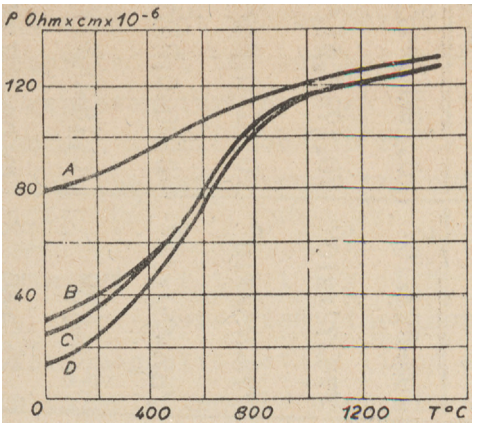

Fig.32. – Resistivity of technical metals in relation to temperature (1)D – mild steel, 2) C – high manganese, 3) B – silicon – manganese steel, 4) A – austenite steel electrode wire).

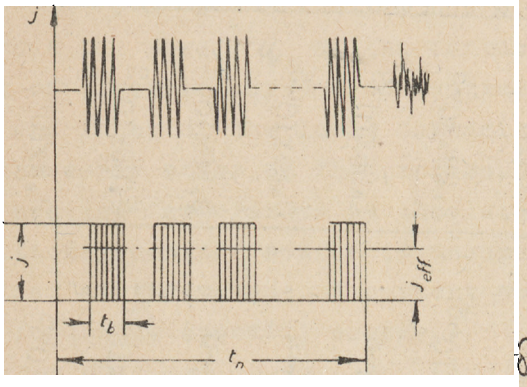

Fig.33. – Scheme of intermittent electric current pre-heat.

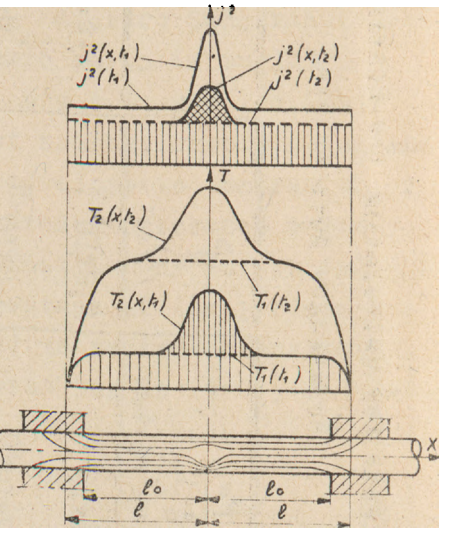

Fig.34. – Temperature distribution over the length of welded rods at an early stage (moment t_1) and to the end (moment t_2) of electric current heating single connection.

In intermittent pre-heating of rods by the electric current (preliminary stage of flash welding) the end-faces are to be periodically connected and broken, usually not less than 3-5 times. In these subsequent connections the electric current undergoes slight change. Thus the process of intermittent pre-heating may be defined according to the scheme for the continuous heating:

a) by the effective electric current averaged for the whole time of the process and having the square-mean density

$$j_{eff} = j \sqrt{\frac{\sum t_{con}}{t_{int}}} \qquad (33)$$

where t_{int} - the total time of the intermittent pre-heating, sec;

$\sum t_{con}$ - summary duration of connection periods, sec. (fig.33);

b) by the contact source having constant specific power, proportional to the voltage drop q_2 across the contacts

$$q_2 = 0{,}24\ U_к\ j_{eff} \qquad (34)$$

The value of $U_к$ is approximately equal to 0.4-0-6v. Higher values of $U_к$ correspond to the intensive spark formation - at low speeds of machine clamp travel- by larger cross - sections of the rods under welding.

Heating scheme in resistance butt welding. In the process of rod heating in the resistance butt welding it is expedient to average the rated temperature of the working parts for the cross-section of the rod. Although the measured temperature irregularity, particularly in the early stage of the process may be rather great, the temperature becomes practically levelled at the later stage of the process. Fot practical ends it is important to estimate the temperature of working ends of the welded rods which are heated by the electric current and from the additional contact source.

The scheme of the infinite rod heated by the constant electric current, uniformly distributed over the

length of the rod, and from the concentrated additional contact source of either instantaneous Q_2 or continuous q_2 action is suitable for such a calculation. This scheme rather well defines the short-term heating process at a high density of electric current in the lengthy rod working ends made of low heat conductive metal.

The temperature T(x,t) of the working ends may be presented by the sum of two temperatures (fig.34)

$$T(x,t) = T_1(t) + T_2(x,t) \qquad (35)$$

1) temperature $T_1(t)$ developed in the heating of infinitely long contactless rod by electric current j passing through resistance ρ which grows linearly with the rise of the temperature (relation 31);
2) temperature $T_2(x,t)$ developed in the local heating of the rod from the additional plane contact source Q_2 or q_2 and by electric current j passing through the resistance which is proportional to the temperature (second member of relation 31).

H e a t i n g o f c o n t a c t l e s s r o d. Temperature of the rod heated by constant electric current j = consta (the resistance of the rod is growing linearly with the temperature rise (31) is expressed through the well known exponentional low (fig.35).

$$\beta T_1(t) = \exp \beta w_0 t - 1 \qquad (36)$$

where $w_0 = 0{,}24 \frac{\rho_0}{(c\gamma)_0} j^2$ – initial rate of heating in °C/sec.

L o c a l h e a t i n g i n r e s i s t a n c e w e l d i n g. Temperature of the local resistance heating of single connected rods is determined for the later stage of the process by the scheme of an instantaneous plane source Q_2 (relation 32) in the infinite rod heated by constant electric current j = const.

$$T_2(x,t) = \frac{Q_2}{c\gamma \sqrt{4\pi a t}} \exp\left(\beta w_0 t - \frac{x^2}{4at}\right) \qquad (37)$$

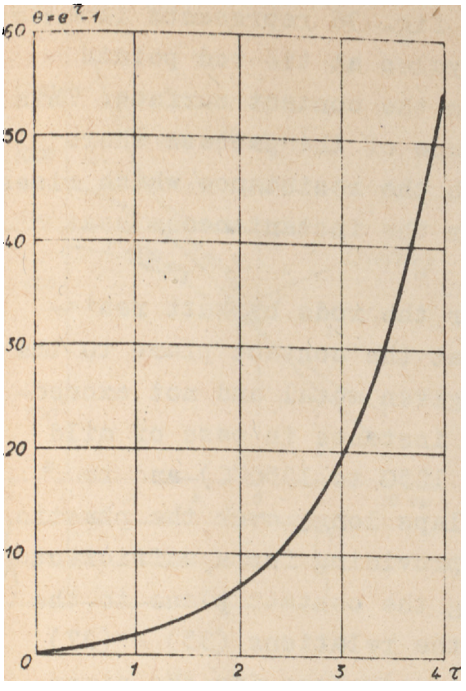

Fig.35. - Exponential rise of temperature in heating of contactless rod with linearly growing resistance by a constant current.

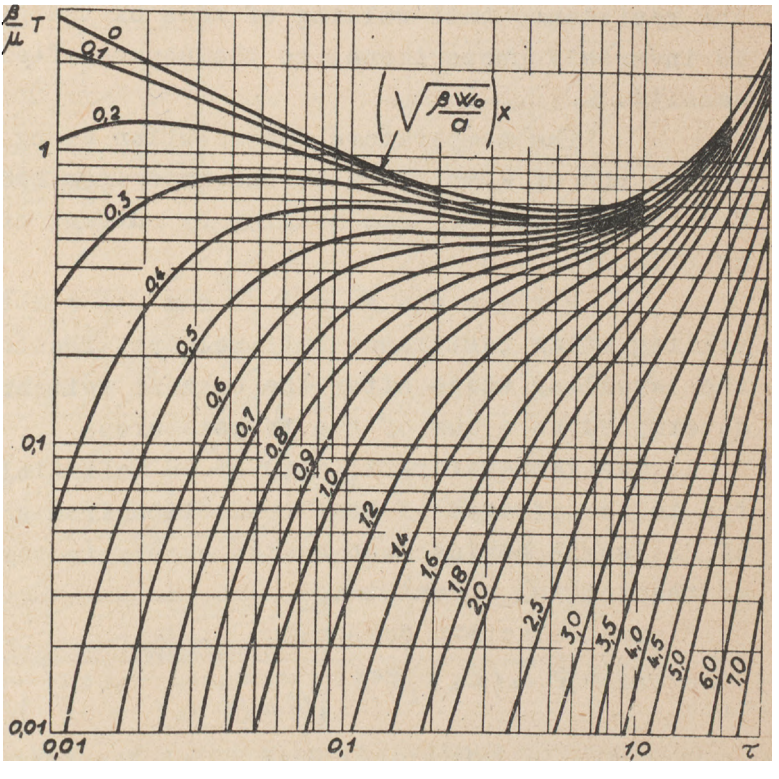

Fig.36. - Local heating of a rod with resistance proportional to temperature by instantaneous heat source Q_2 and constant current j; non-dimensional temperature as a function of non-dimensional time at various values of non-dimensional distance $\sqrt{\frac{\beta w_e}{a}}x$ from the contact.

The nomographic chart in fig. 36 represents in a non-dimensional form the thermal cycles at the rod points located at different distances from the contact surface. This chart discloses the comlicated nature of the process where the electric current passes through the resistance which rises due to the effect of heat flow from the instantaneous heat source Q_2.

In order to weld together the rods by butt resistance method it is necessary to heat the contact plane to the temperature T_k - definite for the given metal and not exceeding its melting temperature - (for instance in case of mild steel this temperature ranges from 1250 to 1350°C) and to heat near- to- the-contact zone 2 laps long, over the plastic deformation temperature T_{pl}, thus providing for a sufficient plastic upset. The time for heating the contact plane to the temperature T_c is calculated from the relations (35) - (37) assuming x=0. The pre-set heating temperature for the given material corresponds to a definite value of product $j^2 t_h$ (see table 5). Hence the necessary duration of the heating in the resistance butt welding of rods of the given material is inversely proportional to the square of electric current density.

The temperature distribution along the length of a welded rod of 25mm diameter and made from 25H3 steel is shown for the end of 12.5 sec heating by current of 25 A/mm^2 density (fig.37).

P r o c e s s o f t e m p e r a t u r e l e v e l l i n g after resistance butt welding. The temperature at the levelling stage after the current switching out may be determined as a sum of two temperatures.

1. The temperature $T_1(x,t)$ of an infinitely long conductive 2ℓ rod in the process of heat conduction from a working section of 2l length having been heated evenly to temperature $T_1(t)$ at the initial moment $t \geq t_h$.

$$T_1(x,t) = \frac{1}{2} T_1(t_h) \left[\operatorname{erf} \frac{x+\ell}{\sqrt{4a(t-t_h)}} - \operatorname{erf} \frac{x-\ell}{\sqrt{4a(t-t_h)}} \right]$$

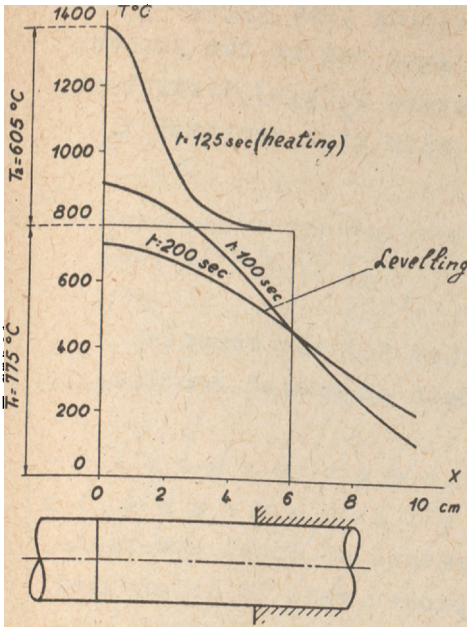

Fig.37. – Temperature distribution over the length of resistance-welded rods at the end of heating t=12.5sec., and in the levelling process t=100 and 200 sec.

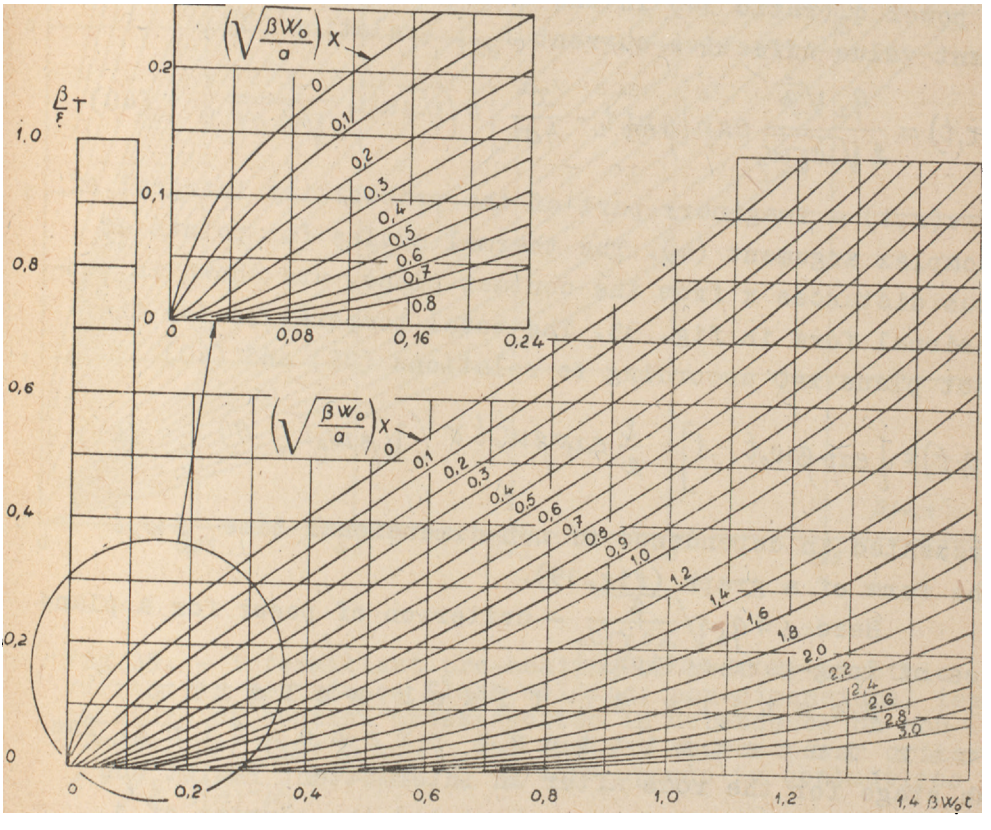

Fig.38. – Local heating of a rod with resistance proportional to temperature by continuous acting plane source q_0 and constant current of j density; non-dimensional temperature $\sqrt{\lambda c \gamma \beta w_0}\,\frac{T}{q_0^2}$ as a function of non-dimensional time $\beta w_0 t$ and non-dimensional distance $\sqrt{\frac{\beta w_0}{a}}\,x$ from the contact.

Here erf.$u = \Phi(u)$ is the error function (see Appendix 1a).

2. The temperature $T_2(x,t)$ of the same rod in the process of heat conduction from local temperature $T_2(x,t)$ distributed according to Gauss' law along axis OX with time constant t_h, is expressed by relation (37)

$$T_2(x,t) = \frac{Q_2}{c\gamma\sqrt{4\pi a t}} \exp\left(\beta w_0 t_h - \frac{x^2}{4at}\right); \quad t \geq t_h \qquad (39)$$

The calculated temperature distribution for the moments t=100 and 200sec, and 12cm rated length of heated section, is shown in graph (fig.37).

L o c a l i n t e r m i t t e n t p r e-h e a t - i n g o f r o d s b y e l e c t r i c c u r r e n t i n f l a s h w e l d i n g. The temperature of local pre-heating for periodically connected and broken rods is determined according to the scheme of the plane source of constant specific power q_2(ratio 34) in the infinite rod heated by a constant value effective current J_{eff} (relation 33)

$$\beta T_2(x,t) = \frac{q_2\sqrt{\beta}}{2\sqrt{\lambda c\gamma w_0}} \exp\left[\beta w_0 t - \frac{x^2}{4at}\right] v\left(\sqrt{\beta w_0 t}, \frac{x}{\sqrt{4at}}\right). \qquad (40)$$

where v(x,t) - imaginary part of the probability integral of the complex argument (4). The thermal cycles for points at various distances x from the contact plane, are shown in non-dimensional form in fig. 38. The total temperature for the contact plane x=0 according to relations (36) and (40)

$$\beta T(0,t) = \left[\exp \beta w_0 t - 1\right] + \frac{\varepsilon}{2} \exp \beta w_0 t\, v\left(\sqrt{\beta w_0 t}; 0\right) \qquad (41)$$

is presented in dependence of non-dimensional time $\beta w_0 t$ in the form of a graph (fig.39).

Here $\varepsilon = q_2\sqrt{\frac{\beta}{\lambda c\gamma w_0}}$ - criterion of power for a plane source of long-term action.

H e a t i n g i n f l a s h w e l d i n g a f t e r i n t e r m i t t e n t p r e-h e a t i n g. The flash stage for the rods after an intermittent resistance pre-heating is usually rather short and the current of j_f density is at this stage - weaker than the effective pre-heat current J_{eff}.

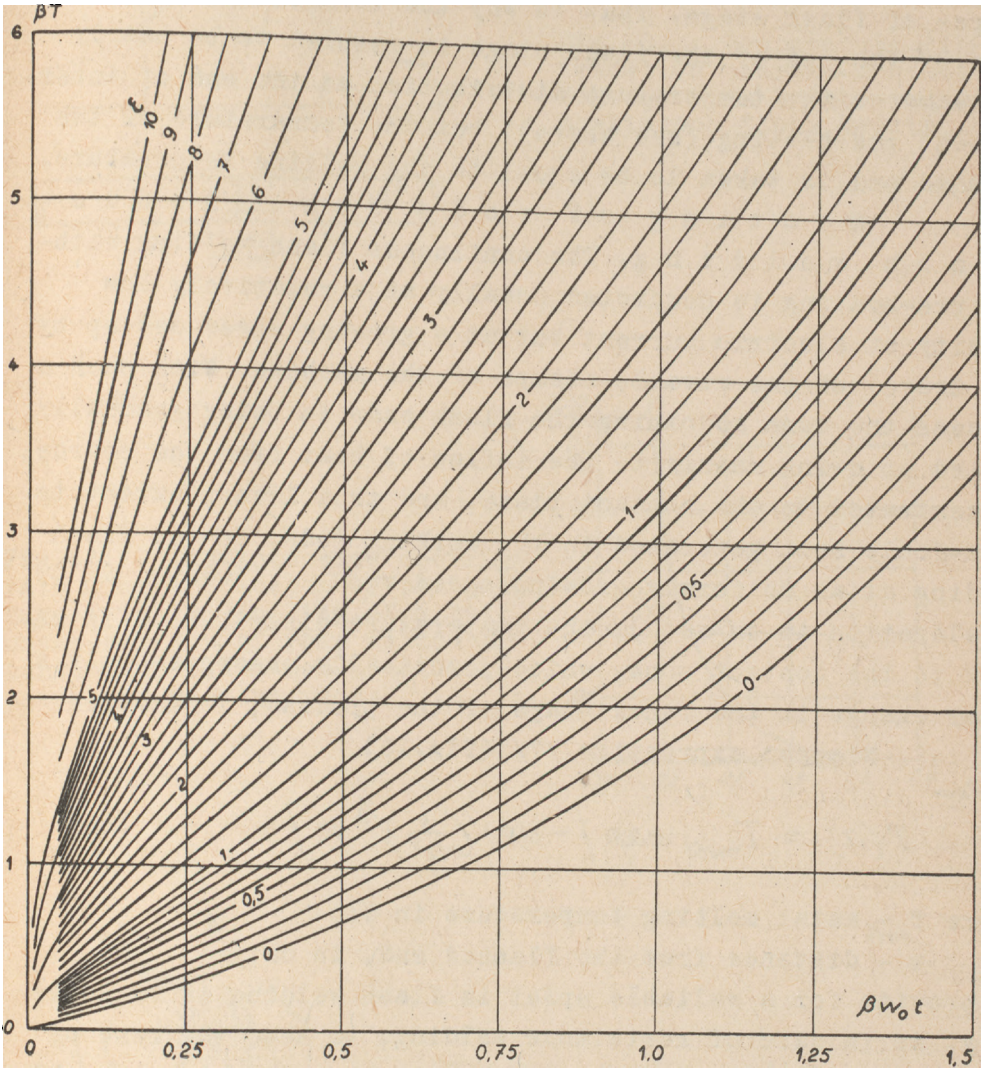

Fig.39. - Intermittent pre-heating of rods by electric current in resistance flash welding; non-dimensional temperature of contact cross-section in dependence on non-dimensional time $\beta w_0 t$ and contact source power criterion $\varepsilon = q_2 \sqrt{\frac{\beta}{\lambda c \gamma w_0}}$; curve $\varepsilon = 0$ corresponds to contactless heating

The rate of flash varies little during the process. It has been experimentally shown that temperature distribution over working sections of the rods, attained at the end of intermittent pre-heating, undergoes little change in the course of flash stage. That is why the temperature distribution by the end of the flash stage is assumed to be nearly the same as the temperature distribution at the end of intermittent pre-heating (see above), but the temperature of the flashed end is taken to be equal to the melting temperature.

H e a t i n g o f r o d s i n c o n t i n u o u s f l a s h w e l d i n g. The continuous flash welding without pre-heating is conducted usually at a relatively low density of electric current but at a growing speed set up by the travel of the movable clamps of the machine. With such a process the zone adjoining the flash ends is being gradually heated up owing mainly to the inflow of heat from the source, concentrated in the contact plane, and to a lesser extent to Lenz-Joule heat generated in the working rods. In the flash welding at an uniformly growing speed $v=st$, (where s - accelaration in cm/sec^2), the temperature distribution in the near to the contact zone, which practically undergoes only a minor change in the final stage of the process, is defined by Nippes' expression /7/ (fig.40)

$$T(x) = T_{melt}\, exp\left[-0{,}92\left(\frac{s}{a^2}\right)^{1/3} x\right]; \qquad (42)$$

where T_{melt} - metal melting temperature in C;

x - distance from the flashed end, in cm;

To provide for a reliable upset in flash welding it is necessary, as in case of resistance welding, to heat the zone of $2\ell_{up}$ length above the temperature T_d. The maximum permissible acceleration S_{max} is determined from the expression (42) as follows:

$$s_{max} = 1{,}3\,\frac{a^2}{\ell_{up}^3}\left(ln\,\frac{T_{melt}}{T_d}\right)^3 \qquad (43)$$

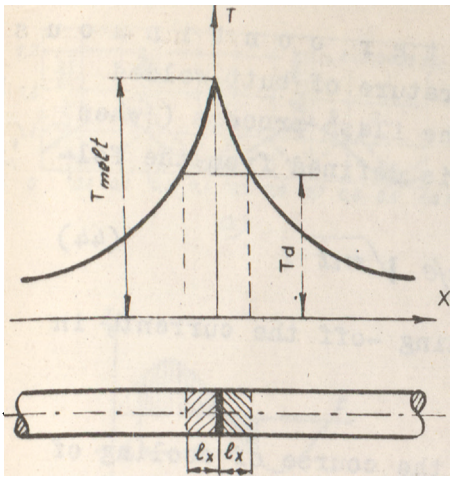

Fig.40. - Temperature distribution near-to-contact zone of rods by the end of continuous flash welding.

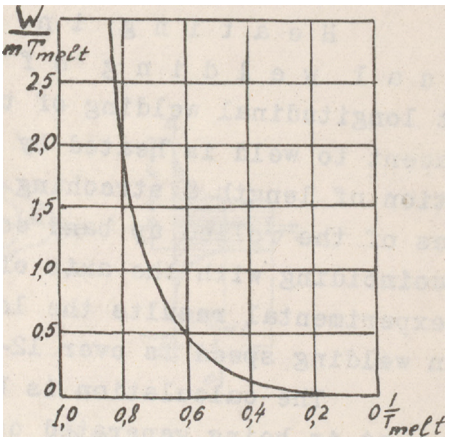

Fig.41. - Instantaneous cooling rate w as a function of temperature T in the cooling of a butt cross-section of rods welded by continuous flash method at an uniformly growing rate.

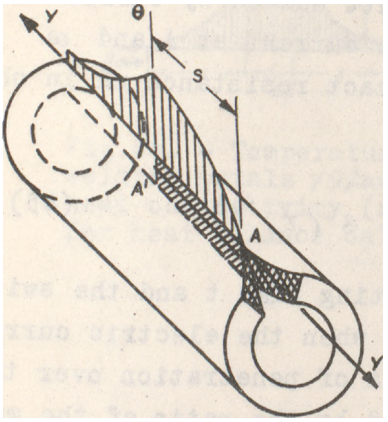

Fig.42. - Scheme of temperature distribution over the butt plane in seam butt longitudinalwelding /8/.

Rod cooling after continuous flash welding. The temperature of butt welded cross-section after completion of the flash process (when the current has been switched off) is defined from the following equation:

$$T(0,t) = T_{melt} \exp mt \operatorname{erfc} \sqrt{mt}, \qquad (44)$$

where t - time elapsed after switching -off the current, in sec;

$$m = 0,85 \left(\frac{s^2}{a}\right)^{1/3} \text{ in sec}^{-1}$$

The instantaneous temperature T in the course of cooling of the welded butt corresponds to instantaneous cooling rate $W^{o}C/sec$ which is taken from the graph in fig. 41.

Heating in seam-butt longitudinal welding of tubes /8/. In the seam-butt longitudinal welding of tubes at speed v the metal zone adjacent to weld is heated by electric current J(t) over a section of length S streching from the point A, where the edges of the rolled up band come into contact, to the point A' coinciding with the axis of electrodes (fig.42). According to experimental results the length S ranges from 8 to 12mm when welding speed is over 12-15m/min.

The calculation is based on the assumption that the heat is being generated on the contact plane as well as in the zone adjacent to weld and then it spreads only in the direction perpendicular to weld (quick-moving source scheme).

The temperature of the butt heated by current $J=J_{max} \times \sin\omega t$(where J_{max} - maximum electric current at A,and ω - angular frequency at average contact resistance mR in ohms is expressed as follows:

$$T(t) = 0,24 \frac{mR_c}{2} I^2_{max} \beta (t_1, t) \qquad (45)$$

Coefficient β depends on the heating time t and the switch-on time t_1 recorded from the moment when the electric current passes zero (fig.43b). The evenness of penetration over the length of the weld may be evaluated by the ratio of the maximum to the minimum temperature (fig.43a).This ratio is closer to

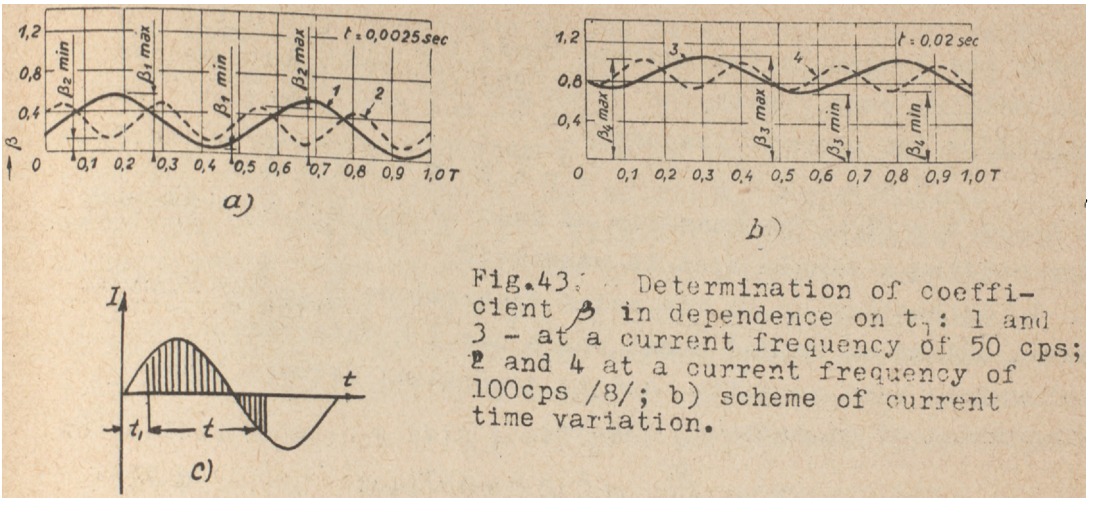

Fig.43. Determination of coefficient β in dependence on t_1: 1 and 3 – at a current frequency of 50 cps; 2 and 4 at a current frequency of 100cps /8/; b) scheme of current time variation.

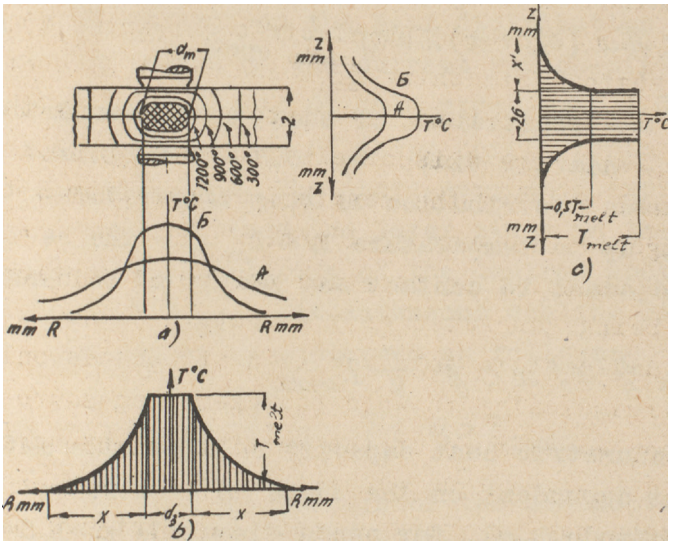

Fig.44. – Temperature distribution in spot welding metals /9/: with high (A) and low (B) heat conductivity (steel); *b* – and *c* – schemes for heat balance calculation.

unity the longer is the heating time, that is the lower is the welding rate V(with the given section length) and the higher is the current frequency.

H e a t i n g i n s p o t w e l d i n g o f s h e e t s /9/. The quantity of heat $Q = Q_1 + Q_2 + Q_3$ necessary for welding a single spot is consumed;

1. In heating up to the rated temperature T_{melt} the central metal column of welded sheet which has 2δ thickness, volumetric heat capacity, and is compressed between the electrodes of diametre d_e(fig.44)

$$Q_1 = \frac{\pi}{4} d_e^2 \, 2\delta c\gamma \, T_{melt} \qquad (46)$$

2. In heating to the temperature 1/4 T_{melt} - the metal ring of width x surrounding the central column.

$$Q_2 = k_1 \pi x \, (d_э + x) \, 2\delta c\gamma \cdot \frac{1}{4} T_{melt} \qquad (47)$$

where $x = 4\sqrt{at}$; a - coefficient of sheet metal temperature conductivity; t - heating time; $k_1 = 0.8$ - coefficient considering the uneven distribution of ring temperature.

3. In heating up to temperature 1/8 T_{melt} - the section of electrodes adjacent to contact and having x^1 thickness

$$Q_3 = 2k_2 \frac{\pi}{4} d_э^2 \, x' c'\gamma' \frac{1}{8} T_{melt} \qquad (48)$$

where $c'\gamma'$ - volumetric heat capacity of electrode metal; k_2 - coefficient dependent on the shape of electrodes: for cylindrical electrode $k_2=1$, for conic electrode $k_2=1.5$ and for spherical contact surface $k_2=2$.

The necessary electric current J_2 in the secondary circuit may be calculated on the basis of the technologically rational welding time t.* Here $Q = Q_1+Q_2+Q_3$ - (see 46 - 48); m - coefficient allowing for the resistance variation during the process of welding; for steels m= 1 - 1,1; for aluminium alloys m= 1.2 - 1.4; $R_{hot} = A_{ok} \frac{\rho_t}{\delta}$ - hot resistance of the welding-circuit section located between the electrodes;

* $$I_2 = \sqrt{\frac{Q}{0{,}24\, m\, R_{hot}\, t}} \qquad (49)$$

ρ_t - specific resistance of the metal heated to a temperature somewhat lower than its melting temperature, (1200 - 1300°C for steel) k=0.8 - 0.9 coefficient accounting for decrease in details resistance due to the current outflow into the less heated zone of the metal; A_0 - coefficient depending on the ratio d_0/δ (fig.45); d_0 - diametre taken as an average value of diametres of the electrode and the spot.

W e l d e d s p o t c o o l i n g in the sheets of thickness δ, after current switching-off and breaking of electrodes, is defined by a scheme of instantaneous normal-circular source in a thin plate with surface heat loss (fig.46).

$$T(r,t) = \frac{Q}{4\pi\lambda 2\delta(t_0+t)} \exp\left[-\frac{r^2}{4a(t_0+t)} - \frac{\alpha t}{c\gamma\delta}\right] \quad (50)$$

Here $Q = Q_1 + Q_2$ - the amount of heat introduced to the sheet metal; t_0 - time constant of a normally distributed heat source, it characterizes the heat distribution along the radius at the moment of the current switch-off; t=0. For instance in welding sheets of mild steel δ= 1.5mm, t_0=0.5 - - 0.9 sec; lesser values of these coefficients correspond to more tough conditions. The above-mentioned expression defines with sufficient accuracy the later stage in the cooling process, where the temperature of the central spot drops to a value below o.5 T_{melt}. Instantaneous cooling rate w °C/sec for the spot center is expressed as follows:

$$w = \frac{4\pi\lambda(T-T_0)^2}{Q/2\delta}; \quad T < 0{,}5\,T_{melt} \quad (51)$$

where T_0 - initial temperature of the sheets to be welded. Instantaneous cooling rate w is inversely proportional to the amount of heat $Q/2\delta$ for the unit of thickness of the welded sheets (see expression 22).

HEATING OF RODS IN FRICTION BUTT WELDING (10/

H e a t s o u r c e. In the friction heating the heat is generated in the thin superficial layer of metal adjoining

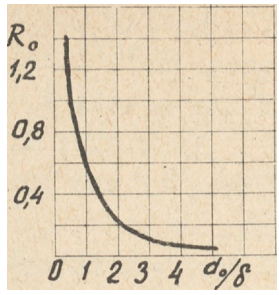

Fig.45. - Diagram of coefficient A_o for determination of initial coefficient of parts in spot welding /9/.

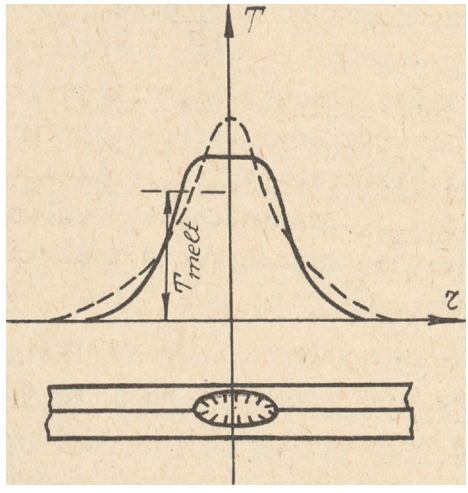

Fig.46. - Temperature distribution at the moment of switching-off the current in spot welding (full line) and equivalent Gaussian temperature distribution (dash line).

the end-faces of rubbing rods. Source thermal power q cal/sec which is equivalent to the instantaneous friction work per unit of time, grows at the initial stage of the process, and after reaching its maximum value drops tending to a stationary value (fig.47a). Specific thermal power q_2 cal/cm^{2}sec of the plane source in the initial stage of the process is unevenly distributed over the rod end-faces, the cross-section outside region being heated faster than the central one. Later on along with the heating of the zone adjacent to the end-face and with the development of upset plastic strains the specific thermal power is levelled over the whole area of the end-faces. For calculating of heating time of friction welding process and of thermal cycle in heat affected zone near to the contact it is permissible to assume the heat source to be evenly distributed over the cross section and constant during working period. The rated power of a plane source is expressed through the following relation:

$$q = kA\,v\,p\,f = k\,\frac{\pi A}{60}\,f\,d\,n\,P \qquad (52)$$

where P – axial compressing force, in kg; n – r.p.m. of the rotating rod; d – diametre (outside) of the rods to be welded, in cm; f – coefficient of sliding friction on the working end-face surfaces; p – pressure in kg/mm^2; v – linear circumferential velocity of the rod in cm/sec; A – thermal equivalent of mechanical work equalling to $2.34.10^{-2}$cal/kg cm; k – coefficient dependent on the distribution pattern of the friction power over the cross-section of the end-face; when the power is uniformly distributed k=1, when the power in a rod grows proportionally to the distance from the centre k=2/3.

The friction coefficient f on the working surface of a given metals' pair depends on the pressure, the linear velocity of the relative travel and the temperature. The coefficient of friction declines with pressure and average linear velocity v rising within certain limits (fig.48).

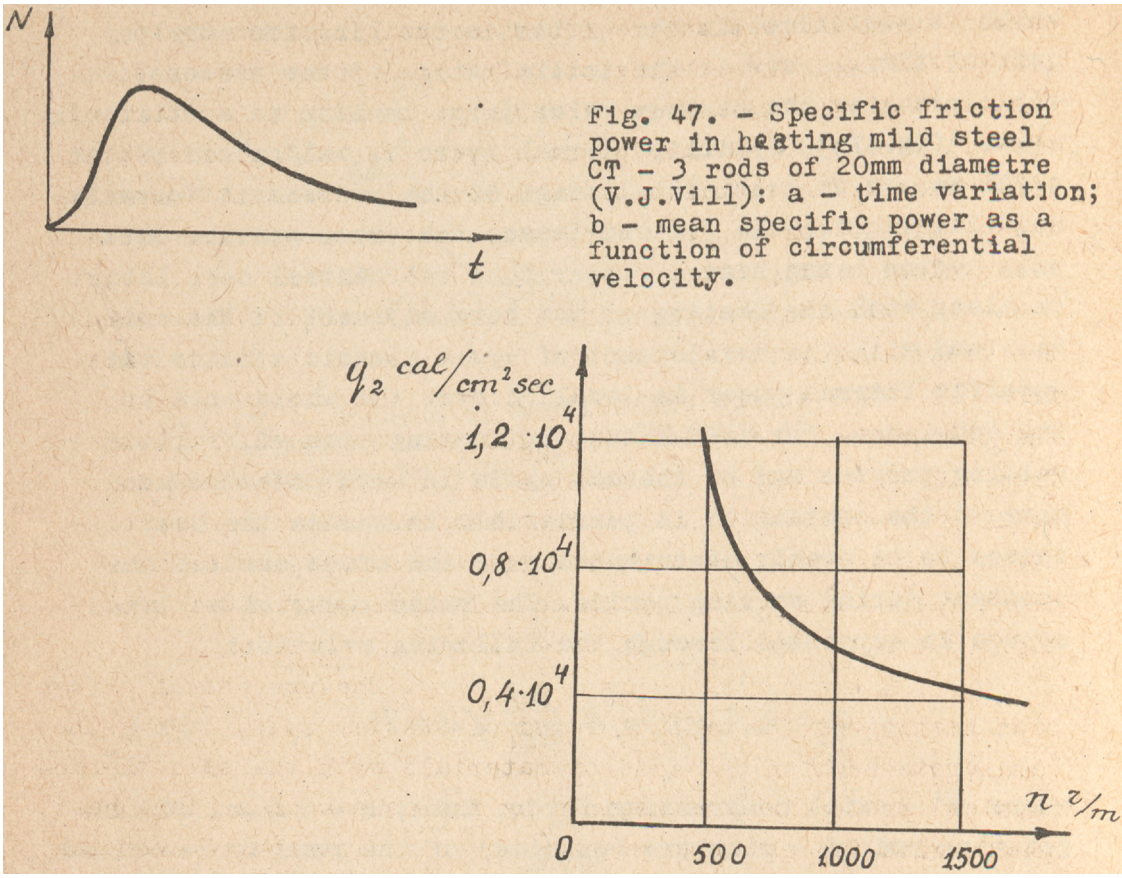

Fig. 47. – Specific friction power in heating mild steel CT – 3 rods of 20mm diametre (V.J.Vill): a – time variation; b – mean specific power as a function of circumferential velocity.

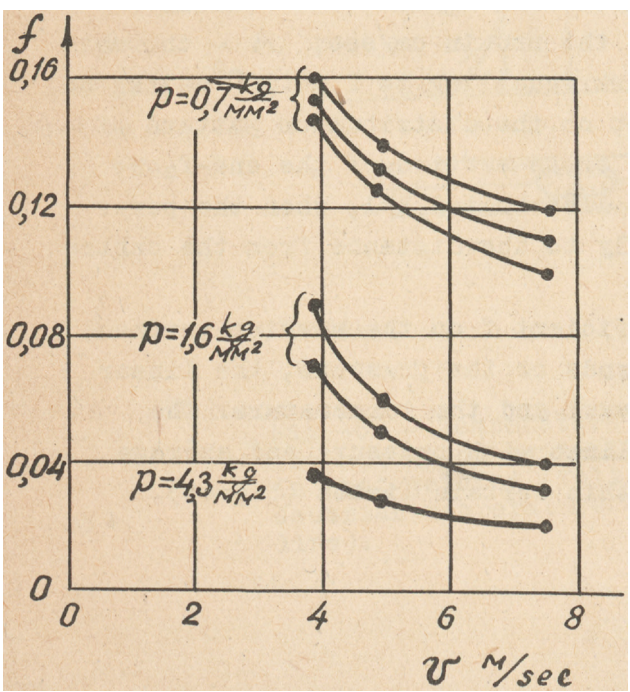

Fig. 48. – Mean friction coefficient in the course of heating tubes of carbon steel 45 and 160/120mm diametre as a function of mean linear velocity v and pressure p (A.S.Gelman and M.P. Sander).

The specific thermal power q_2 of the butt friction of middle carbon steel large diametre tubes is changing from 85 to 150 cal/cm^{2}sec. Thus the friction thermal power cannot be substantiably altered even by varying the main parameters of the friction process throughout a broad technologically available range. The specific thermal power in the friction heating of middle-carbon rods drops with the rise of circumferential velocity (fig.47b).

According to data by R.J.Zakson and V.V.Voznesensky the friction coefficient values in the heating of tubes rise from 0.2 - 0.6 at the beginning of the process to 1 - 2.4 in the process main stage (r.p.m. 200 to 500) specific pressure from 1.2 to 3.8 kg/mm^2. Hence the friction coefficient in welding depends very much on the relative velocity, the specific pressure and the temperature. The aforecited coefficient values f may be used in calculations only under conditions close to those met in experiments.

H e a t i n g p r o c e s s . The process of friction heating of the ends of round or tubular rods, having the same cross-section and made of materials with the same thermophysical properties, is defined by the scheme of a plane heat source with the specific power q_2 evenly distributed over the area of the contact cross-section and remaining constant during the process in an infinitely long rod with superficial heat loss. In heating rods with diameters over 20mm and tubes with wall thickness over 15mm the effect of heat loss may be neglected; the tempareture for these cases is expressed through the following relation:

$$T(x,t) = \frac{q_2\sqrt{t}}{\sqrt{\lambda c\gamma}}\, ierfc\, \frac{x}{2\sqrt{at}} \qquad (53)$$

where $ierfc\, u = \int_u^\infty erfc\, u\, du$ function declining from $\pi^{-1/2} = 0{,}5642$ at $u = 0$ to zero at $u = \infty$ (fig.49).

The contact cross- section temperature for a given material expressed as follows:

$$T(0,t) = \frac{q_2\sqrt{t}}{\sqrt{\pi\lambda c\gamma}} \qquad (54)$$

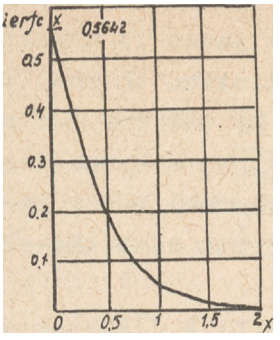

Fig.49. – Integral error function ierfc u.

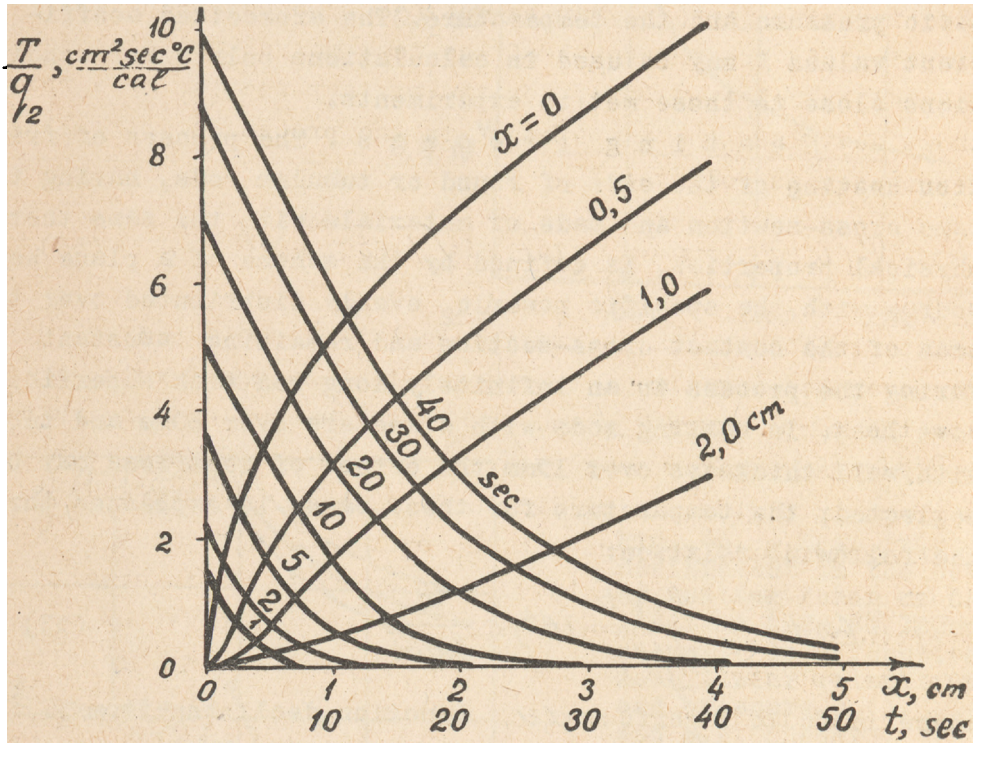

Fig.50. – Heating mild steel rods in end-face friction (λ =0.1 cal/cm sec °C, a=0.08 cm²/sec); isochrones t=const and thermal cycles for x=const.

rises infinitely in proportion with the square root of the time.

The friction heating process for the mild steel rods is represented by the isochrones and the curves of thermal cycle (fig.50). Apparently in the frictional heating of the contact section of welded rods with given metal properties to the pre-set temperature T_c which ensures the sound welding the heating time t_c is inversely proportional to the square of the specific power of the friction

$$q_2^2 t_к = \pi \lambda c \gamma T_к^2 = const \qquad (55)$$

P r o c e s s o f t e m p e r a t u r e l e v e l l i n g. The temperature at the levelling stage upon the termination of heating time lapse t_c may be defined by superposing in expression (6) the processes of the heat source and sink represented by relation (53). For the contact section of a rod without heat loss the temperature in the process of levelling is expressed as follows:

$$T(0,t) = \frac{q_2}{\sqrt{\pi \lambda c \gamma}} \left(\sqrt{t} - \sqrt{t - t_к} \right); \quad t \geq t_к \qquad (56)$$

Characteristics of the thermal cycle in the contact section – the over-heating time t_h above the temperature T which is below the temperature T_c, and the instantaneous cooling rate $^{o}C/sec$ at a given temperature T are to be defined from the graph in fig.51. In welding a metal with given properties and characteristic temperatures the over heating time t_h, as well as the total heating time t_c in welding, is inversely proportional to the square of specific thermal power q_2, while the cooling rate at the given temperature is directly proportional to it.

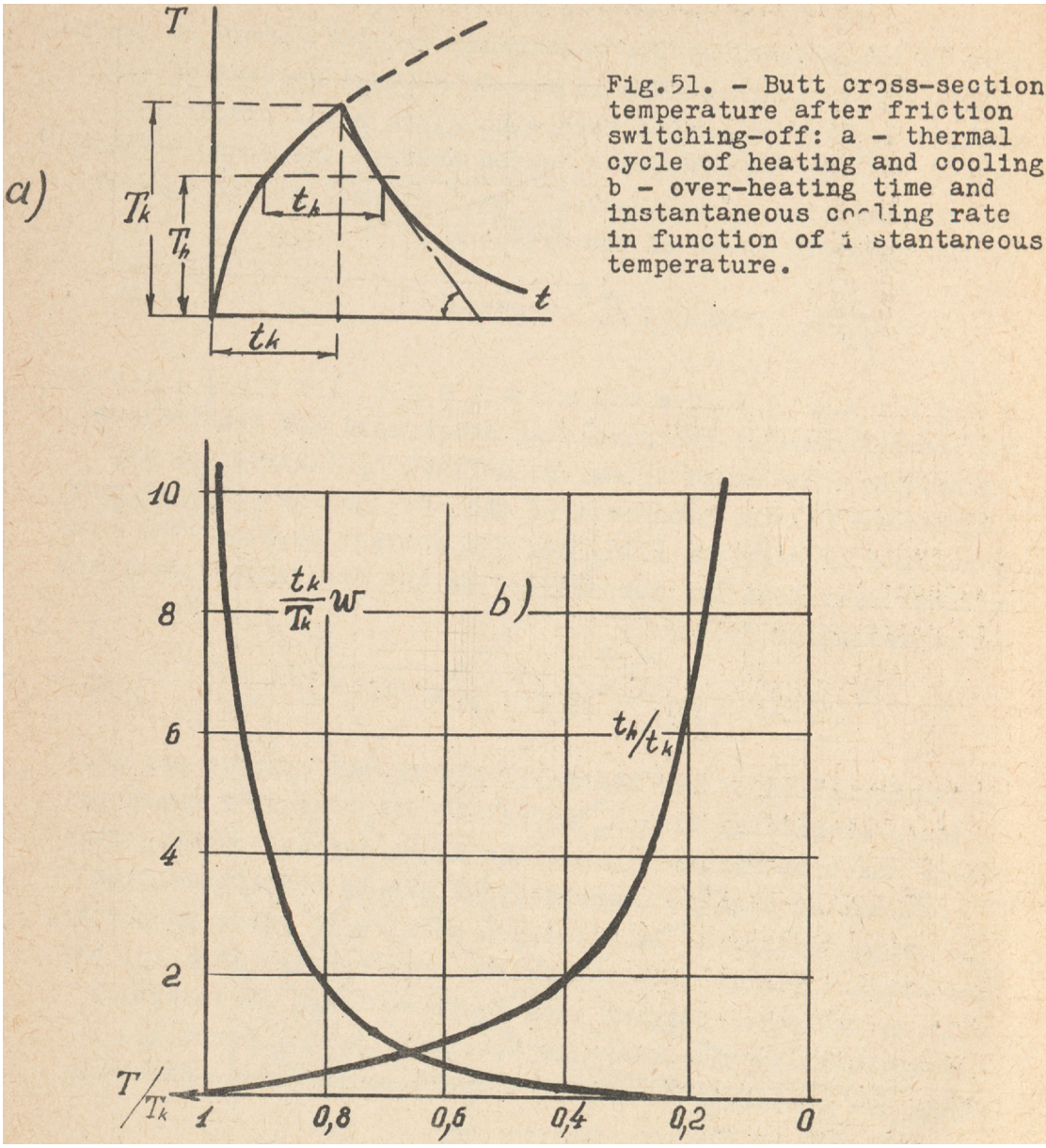

Fig.51. - Butt cross-section temperature after friction switching-off: a - thermal cycle of heating and cooling b - over-heating time and instantaneous cooling rate in function of instantaneous temperature.

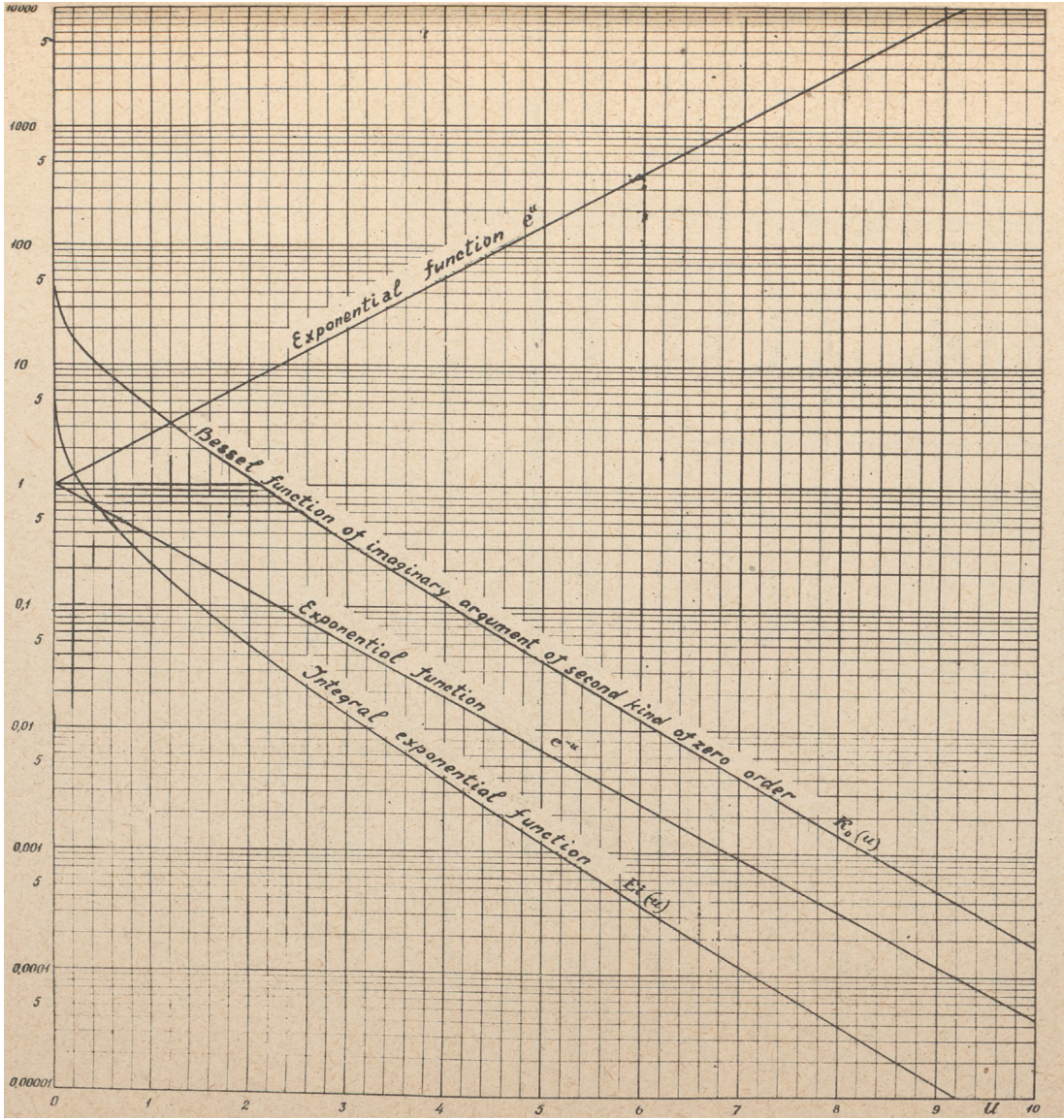

APPENDIX I

Graphs of special functions dealtwith in formulae.

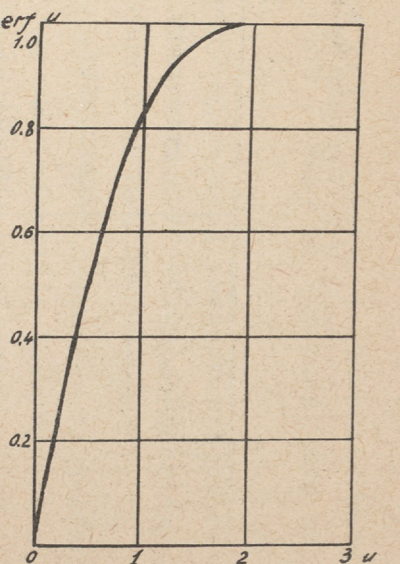

APPENDIX II

Coefficients for Various Metal and Alloys.

Material	Average temperature - T_{av} in ^{o}C	Coefficient of heat conductivity λ in cal/cm sec ^{o}C	Volumetric heat capacity $c\gamma$ in cal/cm^{3} ^{o}C	Coefficient of temperature conductivity a in cm^{2}/sec
Mild steel and low-alloy steels	500–600	0.09–0.1	1.20–1.25	0.075–0.09
Stainless austenite steel	600	0.06–0.08	1.13–1.15	0.053–0.07
Copper	400	0.88–0.9	0.92–0.95	0.95–0.96
Brass	350–400	0.28	0.83	0.34
Aluminium	300	0.65	0.65	0.1
Technical titanium	700	0.04	0.68	0.06

LITERATURE

1. Rykalin N.N., Teplovye osnovy svarki, I (Thermal fundamentals of Welding), USSR Academy of Sciences, Moscow - Leningrad, 1947.

2. Rykalin N.N., Raschjoty teplovykh processov pri svarke (Calculation of Heat Processes in Welding), Mashgiz, Moscow, 1951.

3. Teplovye processy pri svarke (Heat Processes in Welding), Proceedings of Committee for Scientific Development of Electric Welding Problems and Electrothermics, No.2, USSR Academy of Sciences, 1953.

4. Teplovye processy pri kontaktnoj svarke (Heat Processes in Resistance Welding), Proceedings of Metal Welding Laboratory of A.A.Baikov Institute of Metallurgy of USSR Academy of Sciences, Publishing House of USSR Academy of Sciences, Moscow, 1959.

5. Instructions and References on Gas-Flame Treatment of Metals, Heating Metals with Gas Flame, Goschimizdat, 1954.

6. Petrunichev V.A., Distribution of Heat Flow in Submerged Arc Welding, "Svarochnoje Proizvodstvo" (Welding Production) No.4, 1958.

7. Nippes E.F. and others, Welding Journal, No.6, 1955.

8. Zukovsky B.D., Theory of Metal Heating in Seam Butt Longitudinal Welding of Tubes, "Avtogennoje Delo", No.1, 1953.

9. Gelman A.C., Technologija kontaktnoj svarki (Technology of Resistance Welding), Mashgiz, 1952.

10. Articles by V.J.Vill, N.N.Rykalin, A.I.Pugin and V.A. Vasilyeva, A.S.Gelman and M.P.Sander, R.I.Zakson and V.D. Voznesensky (Welding Production), No.10, 1959.

Зак. 37

Ротапринтная ИМЕТ АН СССР